

Deep eutectic solvent fractionation of biomass and development of a multi analytical tools strategy for the characterization of obtained extracts

Auteur : Gebremeskel, Atsbeha Gebreslassie

Promoteur(s) : Richel, Aurore

Faculté : Gembloux Agro-Bio Tech (GxABT)

Diplôme : Master en bioingénieur : chimie et bioindustries, à finalité spécialisée

Année académique : 2024-2025

URI/URL : <http://hdl.handle.net/2268.2/23304>

Avertissement à l'attention des usagers :

Tous les documents placés en accès ouvert sur le site le site MatheO sont protégés par le droit d'auteur. Conformément aux principes énoncés par la "Budapest Open Access Initiative"(BOAI, 2002), l'utilisateur du site peut lire, télécharger, copier, transmettre, imprimer, chercher ou faire un lien vers le texte intégral de ces documents, les disséquer pour les indexer, s'en servir de données pour un logiciel, ou s'en servir à toute autre fin légale (ou prévue par la réglementation relative au droit d'auteur). Toute utilisation du document à des fins commerciales est strictement interdite.

Par ailleurs, l'utilisateur s'engage à respecter les droits moraux de l'auteur, principalement le droit à l'intégrité de l'oeuvre et le droit de paternité et ce dans toute utilisation que l'utilisateur entreprend. Ainsi, à titre d'exemple, lorsqu'il reproduira un document par extrait ou dans son intégralité, l'utilisateur citera de manière complète les sources telles que mentionnées ci-dessus. Toute utilisation non explicitement autorisée ci-avant (telle que par exemple, la modification du document ou son résumé) nécessite l'autorisation préalable et expresse des auteurs ou de leurs ayants droit.

Master thesis report

submitted to obtain the degrees of

Master in Biology AgroSciences (BAS) of the University of Reims Champagne-Ardenne

Master of Science in Engineering of Tallinn University of Technology

Master in Bioengineering: Chemistry and Bioindustries of the University of Liège

Deep eutectic solvent fractionation of biomass and development of a multi analytical tools strategy for the characterization of obtained extracts

Presented by: GEBREMESKEL Atsbeha Gebreslassie

Defended: 25 /06/2025

Supervised by

**Dr VILLAIN-GAMBIER Maud at Institut Pluridisciplinaire Hubert Curie IPHC
located at 23 rue du Loess, 67200 Strasbourg, France**

from: 03/03/2025 to 29/08/205

**Bioceb supervisors: RICHEL Aurore, University of Liège; KARPICHEV Yevgen,
Tallinn University of Technology**

Confidentiality: No

Abstract

The increasing demand to replace chemicals derived from fossil fuels with sustainable ones has positioned lignocellulosic biomass as a promising alternative. Among its components, lignin is the most underutilized despite being rich in aromatics. In this work, the extraction of lignin from brewery spent grain using deep eutectic solvents (DES) and its electrochemical depolymerization is studied. Two extraction temperatures (100 or 140°C) were investigated. The DESs studied were choline chloride/lactic acid (ChCl/LA) at a molar ratio of 1:1 and 1:10, and a ternary DES composed of choline chloride, ethylene glycol, and oxalic acid (ChCl/EG/OA). Kamlet-Taft parameters of the DESs were also determined using solvatochromic dyes to. for the ChCl/LA based extraction, the results revealed that both acidity (high LA content) and high temperature favored solid recovery whereas their effect on lignin purity wasn't as visible. The ternary DES system yielded the least pure lignin despite its high solid recovery. These observations were in line with the Kamlet-Taft parameters of the DES. The difference between the acidity and basicity ($\alpha - \beta$) of DESs as determined using solvatochromic dyes gives an insight into lignocellulose solvation potential. High values mean better the DES dissolves lignin better. The $\alpha - \beta$ value for the three DESs were: ChCl/LA 1:10) > ChCl/LA (1:1) > ChCl/EG/OA (1:2:10 w%). The structural analysis of the recovered lignin was also analyzed using FTIR and 2D HSQC NMR. FTIR spectra showed characteristic bands for aromatic skeletal vibrations (~ 1510 and 1630 cm^{-1}). NMR analysis confirmed the presence of guaiacyl (G) and syringyl (S) units as well as linkages such as β -O-4, β - β . Finally, electrochemical depolymerization of the extracted lignin in alkaline media using a nickel working electrode was researched. The lignin sample that was extracted with ChCl/LA (1:1) at 140°C for 3h was studied for depolymerization, and preliminary results demonstrated that lignin breakdown under mild, reagent-free conditions, as observed by its color change and reduced UV absorbance after electrolysis. This is an interesting starting point to proceed further with the identification and quantification of the monomers.

Key words: deep eutectic solvent, extraction, lignin, lignocellulosic biomass, depolymerization

Table of Contents

Abstract.....	II
Table of Figures	V
List of Tables.....	VI
List of abbreviations.....	VII
1 Introduction	1
1.1. Context	1
1.2. Objectives.....	2
2 Literature Review	3
2.1. Lignocellulosic biomass	3
2.1.1. Cellulose	4
2.1.2. Hemicellulose	4
2.1.3. Lignin	4
2.2. Lignin first biorefinery.....	7
2.3. Methods of biomass fractionation.....	8
2.3.1. Biomass fractionation with deep eutectic solvents	9
2.3.2. Tailoring lignin properties through solvatochromic tuning of deep eutectic solvents 14	
2.4. Lignin depolymerization.....	16
2.4.1. Thermal depolymerization	16
2.4.2. Chemical depolymerization	16
2.4.3. Reductive and oxidative depolymerization	17
2.4.4. Biological depolymerization	18
2.4.5. Electrochemical depolymerization.....	18
3 Materials and Methods.....	20
3.1. Materials.....	20
3.2. Methods.....	20
3.2.1. Biomass pretreatment.....	20
3.2.2. DES preparation.....	22
3.2.3. Extraction	22
3.2.4. Determination of DES Kamlet-Taft parameters	24
3.2.5. FTIR spectroscopy	25
3.2.6. NMR spectroscopy	25
3.2.7. Klason lignin.....	26

3.2.8.	Protein content	27
3.2.9.	Electrochemical depolymerization	27
3.2.10.	Size exclusion chromatography	28
4	Results	29
4.1.	Visual characteristics and Kamlet–Taft parameters of DESs.....	29
4.2.	Extraction results	31
4.2.1.	Lignin rich fraction	31
4.2.2.	Cellulose rich fraction.....	33
4.2.3.	FTIR spectra	33
4.2.4.	NMR spectra.....	34
4.3.	Electrochemical depolarization.....	36
5	Discussion of results.....	38
5.1.	Effect of extraction conditions on lignin yield	38
5.2.	Structural features of lignin	38
5.3.	Electrochemical depolymerization of lignin	39
6	Conclusion and feature perspectives	41
7	References	42

Table of Figures

Figure 1: APROV(E) project	1
Figure 2: graphical representation of the objectives in this work.....	2
Figure 3: Complex lignocellulosic biomass.....	3
Table 1: Different lignocellulosic biomasses and their major components(Yousuf et al., 2019)4	
Figure 4: lignin subunits and interunit linkages (Zhang, 2022).....	5
Table 2: Lignin sub-unit composition of different biomasses	6
Figure 5: different methods for isolating lignin from lignocellulosic biomass adopted from (Sun et al., 2018)	9
Figure 6:I) binary phase diagram for eutectic mixtures II) Phase change for Choline chloride/urea as a function of mole fraction	10
Figure 7: Combinations of hydrogen bond acceptors (HBAs) and hydrogen bond donors (HBDs) (Chen et al., 2020b).....	10
Table 3: Extraction conditions, yield and purity of different DESs.....	13
Figure 8: Kamlet-Taft parameters of different DESs and their relationship with lignin solubility (a-c) and xylan solubility (d-f) adopted from (Zhang et al., 2023a)	15
Figure 9: Depolymerization of DES-extracted lignin by hydrogenolysis ; depolymerization conditions (200 mg DES fractionated lignin, 200 mg Ru/C (5 wt% Ru loading), 20mL methanol, 18 h); Abbreviations : DPL= Derivatization protection Lignin (extracted by Derivatization protection DES =ChCl/EG/OA), CSL = cleavage stabilization Lignin (extracted by cleavage stabilization DES= ChCl/OA); the numbers in DPL10 and CSL80 refers to %w of OA and EG in the ternary DES respectively.....	17
Figure 10: Schematic of electrochemical membrane (AEM: Anion Exchange Membrane, NFM: Nanofiltration Membrane)(Stiefel et al., 2015)	18
Figure 11: Schematic of a soxhlet extractor.....	21
Table 3: % of extractables (g/g) removed in each stage of Soxhlet extraction	21
Table 4: Quantities of pure components required to prepare 100 g of DES	22
* T _m is the melting temperature of compound, HBA = hydrogen bond acceptor, HBD = hydrogen bond donor,.....	22
Table 6: Protein content of different samples as determined by the CHN elemental analysis .	27
Figure 13: Color change of solvatochromic dyes in the studied DESs and methanol	30
Figure 14: Kamlet-Taft parameters of the studied DESs. The term in paranthesis is the molar ratio of the components	30
Figure 15: Lignin extraction from brewery spent grain with different DES at 100 and 140 °C: a) solid recovery b) purity c) lignin yield ; Note that purity and yield of AG5-L was not determined.....	32
Figure 16: Cellulose rich residue obtained after lignin extraction with different DESs at 100 or 140°C.....	33

Figure 17: FTIR spectra of different lignin extracted with different DES at 100 °C or 140 °C	34
Figure 18: NMR spectra of lignin extracted at 140 °C with ChCl/LA having molar ratio of (a) 1:10 (AG4-L) and b) 1:1 (AG6-L).....	35
Figure 19: Comparing before and after electrochemical depolymerization AG6-L (ChCl/LA (1:1) , 140°C: 3h): a) color change, b) UV absorbance, c) SEC elution profile as a function of retention time	37

List of Tables

Table 1: Different lignocellulosic biomasses and their major components	4
Table 2: Lignin sub-unit composition of different biomasses	6
Table 3: % of extractables (g/g) removed in each stage of Soxhlet extraction	21
Table 4: Quantities of pure components required to prepare 100 g of DES	22
Table 5: The studied Extraction conditions.....	24
Table 6: Protein content of different samples as determined by the CHN elemental analysis .	27

List of abbreviations

BSG	Brewery Spent Grain
CHN	Carbon, Hydrogen, Nitrogen (elemental analysis)
DES	Deep Eutectic Solvent
DMSO	Dimethyl sulfoxide
FTIR	Fourier-Transform Infrared Spectroscopy
G	Guaiacyl
H	p-Hydroxyphenyl
HBA	Hydrogen bond acceptor
HBD	Hydrogen bond donor
HSQC	Heteronuclear Single Quantum Coherence
LCB	Lignocellulosic biomass
NMR	Nuclear Magnetic Resonance
S	Syringyl
SEC	Size Exclusion Chromatography
UV-Vis	Ultraviolet-visible

1 Introduction

1.1. Context

This work is part of the broader APROV(E) project (“Assembly of green PROcesses for optimal biomass Valorization”), which aims to develop a circular biorefinery for the efficient valorization of lignocellulosic biomass (LCB). The different aspects of the APROV(E) projects are depicted in Figure 1. The emphasis of this work is on work package one (WP1) that is to select, design, and optimize DESs for effective biomass fractionation. A lignin first biorefinery approach was adapted to extract lignin suitable for electrochemical depolymerization in work package two (WP2) while generating cellulose and hemicellulose-rich fractions suitable for downstream processing in work package four (WP4). This work also includes preliminary studies of the electrochemical depolymerization of extracted lignin in WP2.

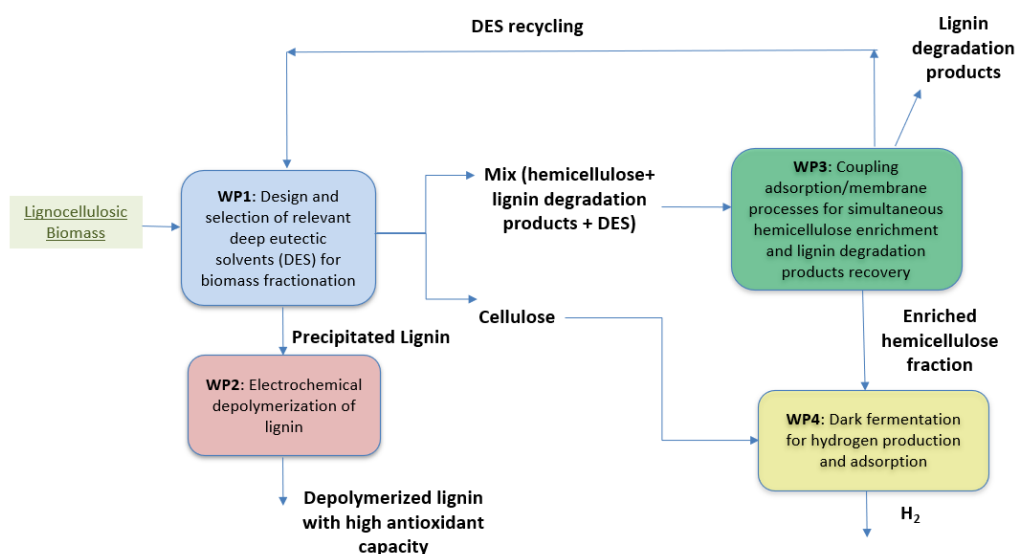


Figure 1: APROV(E) project

LCB is recognized as a renewable resource to produce fuels, chemicals, and material. It is estimated that around 180 billion tons of LCB is produced annually worldwide ((Mujtaba et al., 2023). It is primarily composed of cellulose, hemicellulose, and lignin. The valorization of cellulose and hemicellulose is industrially mature. However, lignin remains underutilized despite being the number one natural source of aromatic compounds (Kropat et al., 2021). This underutilization largely stems from the recalcitrant and heterogeneous nature of lignin as well as from the structural modifications that occur during conventional pretreatments such as kraft which lead to condensation or loss of reactive β -O-4 linkages (Cassoni et al., 2022).

As a result, interest has grown in lignin-first biorefinery approaches that prioritize lignin stabilization to preserve its native structure (Luo et al., 2023). Deep eutectic solvent (DES) fractionation of biomass is an emerging method in this aspect. DESs are formed by mixing hydrogen bond donors (HBDs) and hydrogen bond acceptors (HBAs) and are interesting for biomass fractionation due to their tunability, low toxicity, and capacity to selectively solubilize lignin while preserving labile linkages. Nevertheless, a deeper understanding of how DES composition influences extraction efficiency and lignin structure is required. This study is a step in that direction.

The report starts with a literature Review contextualizing the different aspects of the project. It introduces lignocellulosic biomass describing its components and going deeper with lignin as it is the component of interest in this project. It then discusses the different available methods of biomass valorization. DESs are given special attention. Approaches on how to tailor lignin structure are emphasized. It then follows up with a discussion on lignin depolymerization. The second part of the report is a materials and methods section detailing DES preparation, biomass pretreatment, lignin extraction, and different characterization methods (FTIR, NMR, Klason, SEC). Finally, a method on electrochemical depolymerization of lignin is presented. The third part of the report presents the results of the work. A fourth part is dedicated to discussions to critically analyze results and compare them with literature. The work finishes with a conclusion and future perspectives section summarizing the important findings and giving insights into future work.

1.2. Objectives

The study aims to isolate lignin samples with varying structural characteristics from brewery spent grain for evaluation in electrochemical depolymerization. Figure 2 depicts the objectives graphically. The study aims to achieve this by selecting, synthesizing, and characterizing DESs and using different temperatures for extraction. In particular, this study aims to:

- Select and synthesize DESs suitable for lignin extraction
- Determine the Kamlet-Taft parameters of the synthesized DESs
- Extract lignin from brewery spent grain using the selected DESs at 100 or 140°C
- Characterize extracted lignin with FTIR, NMR, and Klason
- Depolymerize lignin using electrochemical cells.

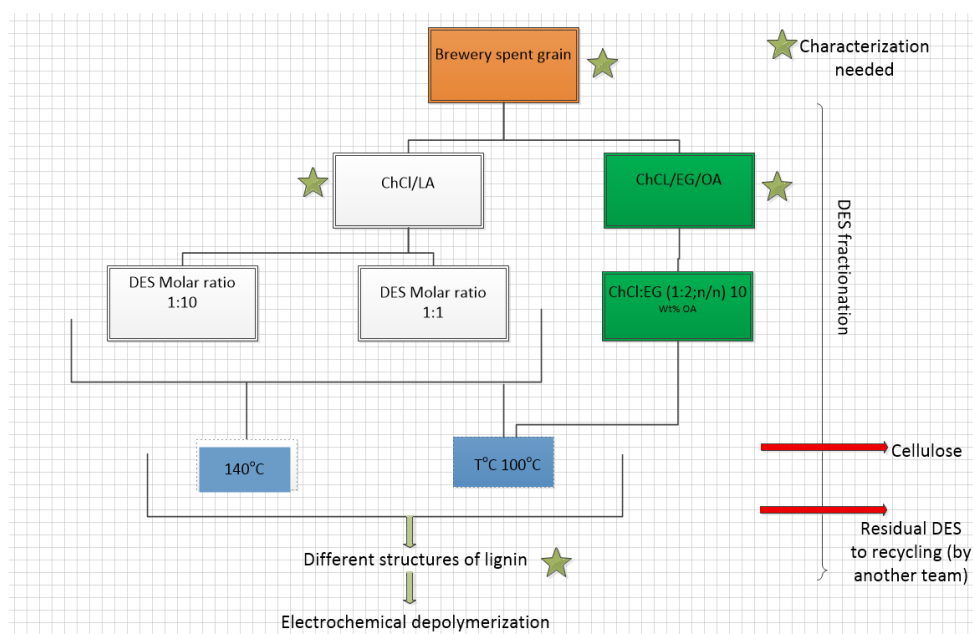


Figure 2: graphical representation of the objectives in this work

2 Literature Review

2.1. Lignocellulosic biomass

Most of our chemicals are derived from fossil resources such as petroleum, coal, and natural gas. These resources are finite, are unequally distributed in the world, and have severe environmental consequences. This makes the search for renewable substitutes a hot agenda globally (Zhang, 2022). Lignocellulosic biomass represents the most abundant renewable organic resource on Earth with an estimated production of 180 billion tons annually. It comes in different forms such as agricultural and forest residues, energy crops, and grass (Mujtaba et al., 2023). It is primarily composed of cellulose, hemicellulose, and lignin. These three structural components form a highly ordered and recalcitrant matrix in plant cell walls (Figure 3), enabling mechanical support and resistance to microbial degradation (Luo et al., 2023). Depending on its origin, lignocellulosic biomass can be categorized softwood, hardwood, and herbaceous biomass. Softwood, predominantly coniferous trees, contains a high proportion of guaiacyl (G) lignin, while hardwoods, such as deciduous trees, have a mixture of syringyl (S) and guaiacyl units. Herbaceous biomass, including grasses and agricultural residues, has a more diverse lignin composition with hydroxyphenyl (H) units alongside G and S subunits, making it structurally distinct from woody biomass (Korányi et al., 2020).

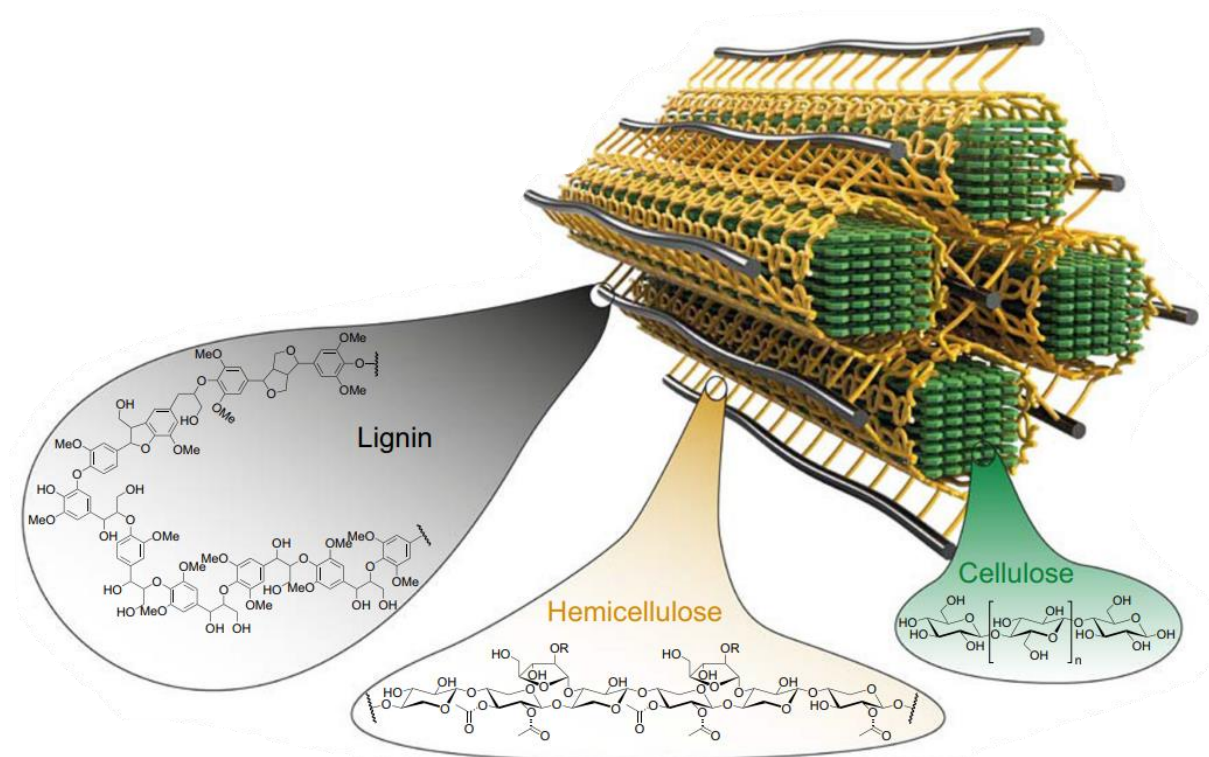


Figure 3: Complex lignocellulosic biomass

Table 1 presents typical compositions ranges of cellulose, hemicellulose, and lignin in various lignocellulosic biomasses (Yousuf et al., 2019). The cellulose content varies widely across the feedstocks, from 21–54% in energy crops to 45–55 % in hardwoods. Hemicellulose is most abundant in grasses (25–50%) and least in energy crops (5–30 %). Lignin content is lowest in energy crops (5–10%) and highest in softwoods (25–35 %).

Table 1: Different lignocellulosic biomasses and their major components (Yousuf et al., 2019)

Raw material	Cellulose (%)	Hemicellulose (%)	Lignin (%)
Energy crops	21-54	5-30	5-10
Grasses	25-40	25-50	10-30
Softwood	45-50	25-35	25-35
Hardwoods	45-55	24-40	18-25

2.1.1. Cellulose

Cellulose, the most abundant biopolymer on earth, is the major structural component of plant cell wall. Its composition varies between species reaching as high as 90% in cotton. Structurally, cellulose is a linear homopolymer of β -D-glucose units linked by β -(1 \rightarrow 4) glycosidic bonds that form long chains that are bundled into microfibrils through hydrogen bonding and van der Waals interactions. These microfibrils have both crystalline and amorphous regions. The crystalline part is enzymatically resistant, while the amorphous part is easily hydrolysable (Bajpai, 2016). The degree of crystallinity is a critical factor affecting enzymatic digestibility during biomass conversion processes.

2.1.2. Hemicellulose

Hemicellulose is a heterogeneous polysaccharide that comprises 20–50% of lignocellulosic biomass by dry weight, depending on the source (Bajpai, 2016). It is composed of pentose sugar monomers such as xylose and arabinose with hexoses such as mannose and galactose, often linked via β -(1 \rightarrow 4) and β -(1 \rightarrow 3) glycosidic bonds. Unlike cellulose, hemicellulose is amorphous and branched. This structural diversity makes hemicellulose more susceptible to chemical and enzymatic hydrolysis compared to cellulose (Yousuf et al., 2019). Their removal during pretreatment is essential to improve cellulose accessibility in biofuel production. In biorefinery applications, hemicellulose-derived pentoses are important feedstocks for the production of furfural, xylitol, and second-generation ethanol (Liu et al., 2018). Hemicellulose can also be chemically modified for advanced biomaterials. For instance, esterification and etherification techniques enable the creation of thermoplastic films, hydrogels, and packaging materials (Mujtaba et al., 2023).

2.1.3. Lignin

Lignin is the second most abundant component of lignocellulosic biomass next to cellulose comprising 10–35% of the lignocellulosic biomass (Bajpai, 2016) and nearly 30% of the organic carbon in the biosphere (Kropat et al., 2021). It is highly complex and recalcitrant. Its main role is to protect the other lignocellulosic components from microbial biodegradation, make the plant cell wall hydrophobic and strong. It is the largest pool of aromatic compounds on earth (Wang et al., 2020).

Lignin comes from different sources such as agricultural-waste, food waste, forest residue, and the pulp and paper industry (Cassoni et al., 2022). The global pulp and paper industries alone produce over 70 million tons of lignin annually during the pulping process, which is designed

to separate cellulose fibers from plant material. The majority of this lignin is typically burned to sustain the energy needs of the process. Only about 2% of it is being utilized for high-value applications (Chen et al., 2023). With growing interest in sustainable biorefineries, valorization of lignin into value-added products is receiving increasing attention (Ragauskas et al., 2014).

Although the true structure of lignin is not fully known since its isolation involves harsh conditions that alter its structure in the process (Khalili et al., 2021), it is well-accepted that it is a cross-linked polymer of three monomers namely p-hydroxyphenyl (H-unit), guaiacyl (G-unit), and syringyl (S-unit) (Ruwoldt et al., 2023). The structure of the three monomers is depicted in Figure 4. It is a heterogeneous and highly branched aromatic polymer. The primary inter monomer linkages include (Chen et al., 2023; Ralph et al., 2019) (see Figure 4).

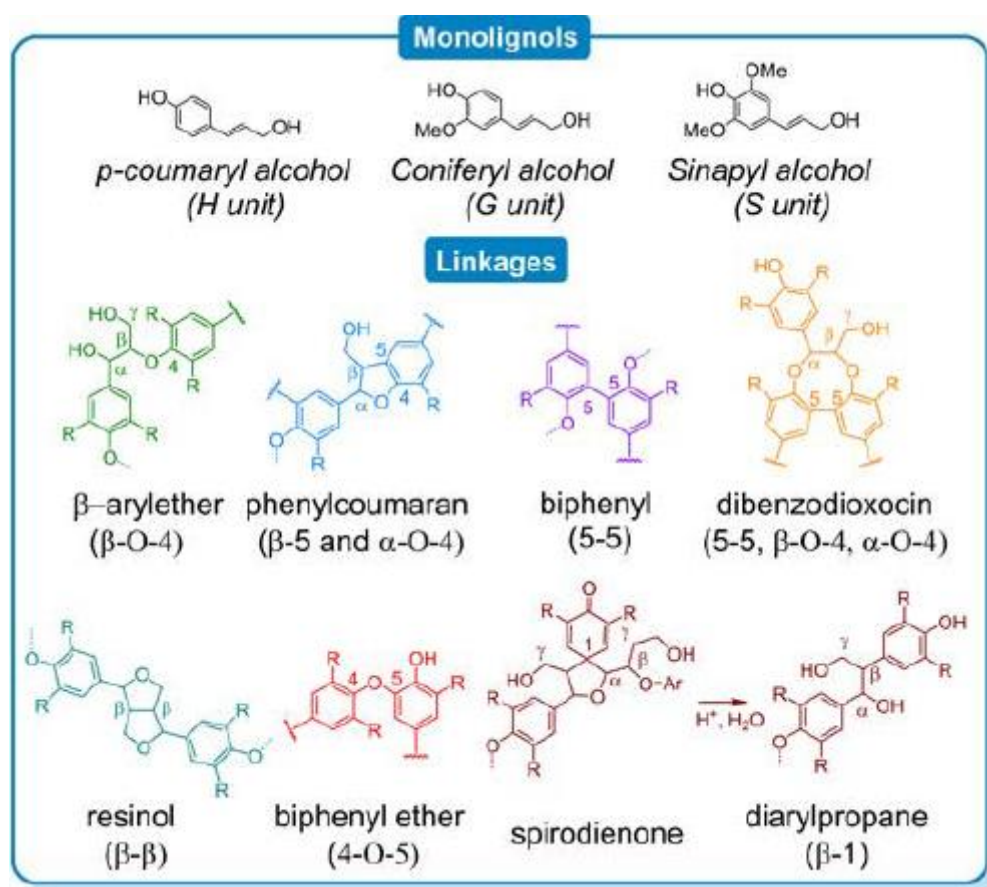


Figure 4: lignin subunits and interunit linkages (Zhang, 2022)

- **β -O-4 (aryl ether)**: the most abundant linkage constituting up to 60% of native lignin. It connects the β -carbon of the alcohol group in one monolignol to the oxygen of the aromatic ring in another, forming a bridge-like structure.
- **β - β (resinol), β -5 (phenylcoumaran), β -1 (spirodienone)**
- **5-5 and 4-O-5 (biphenyl ether and diaryl ether) linkages**.

The composition of lignin monomers differs from plant to plant. Softwoods, such as pine and spruce, are characterized by a higher G-unit content (up to 90–95%). This results in a highly cross-linked structure rich in carbon–carbon bonds, which limits its depolymerization efficiency (Feofilova and Mysyakina, 2016). Hardwoods like oak and eucalyptus typically contain both G and S units in nearly equal proportions, often with an S/G ratio ranging from 0.5 to 2.0, and negligible H units. The higher proportion of S units, which possess two methoxy groups, leads to fewer C–C linkages and a higher abundance of β -O-4 ether linkages, enhancing chemical reactivity and making hardwood lignin more suitable for depolymerization into monomers (Cassoni et al., 2023a; Ralph et al., 2019). Additionally, certain non-woody plants, such as grasses, tend to include all three (H, G, and S), (Lourenço et al., 2016), often with additional hydroxycinnamates such as ferulates and p-coumarates (Provost et al., 2022). Grasses exhibit higher prevalence of S units compared to other plants. Other specialized forms like C-lignin, composed of caffeyl alcohol, occur in certain seed coats and exhibit a linear benzodioxane structure (Chen et al., 2023; Wang and Deuss, 2023).

Effort is ongoing to valorize lignin to value added compounds and bio-based materials to exploit its valuable functional properties such as antioxidant activity, UV protection, and

Table 2: Lignin sub-unit composition of different biomasses

Biomass	H (%)	G (%)	S (%)	Reference
Softwood (spruce/pine)	<5	90-95	<5	(Provost et al., 2022)
Hard wood (olive tree pruning)	0-5	40-60	40-60	(Cassoni et al., 2023a)
Crops (brewer's spent grain)	10	50	40	(Provost et al., 2022)
Monocot grasses (wheat/maize/rice)	5	70	25	Feofilova et al., (2016)
Sugarcane bagasse	2	38	60	(Mujtaba et al., 2023)
Miscanthus \times giganteus	4	52	44	(Yousuf et al., 2019)

antimicrobial behavior (Mujtaba et al., 2023). However, a set of factors are contributing to the underutilization of lignin. One major obstacle lies in the heterogeneous and irregular structure of lignin. Unlike cellulose and hemicellulose, which have more uniform and predictable structures, lignin exhibits significant variation in its composition and bonding patterns, which make it challenging to process and modify with precision ((Sethupathy et al., 2022). Lignin's recalcitrance to systematic depolymerization is another significant challenge. Efficiently breaking down lignin into its constituent monomers for further processing has proven to be a complex task. The intricate network of covalent bonds within lignin requires advanced and often energy-intensive depolymerization techniques. During lignin degradation processes, such

as pyrolysis or enzymatic treatments, the production of a complex mixture of aromatic compounds further complicates its utilization. The resulting mixture can be challenging to separate and refine, limiting the ability to obtain specific, high-value compounds. This complexity in the degradation products adds a layer of difficulty to the downstream processing and utilization of lignin-derived materials (Zhang et al., 2020). Another barrier to the extensive use of lignin is its dark color, often referred to as the ‘color problem’. The dark pigmentation arises from the complex aromatic structures within lignin, making it less aesthetically appealing and more challenging to incorporate into light-colored products. The color issue poses a hurdle for applications where visual appeal is critical.

2.2. Lignin first biorefinery

Traditional biorefineries focus on the valorization of cellulose and hemicellulose. In these processes lignin is often degraded due to harsh chemical or thermal treatments, such as kraft or acid hydrolysis processes, which result in a highly condensed, structurally modified lignin that is poorly suited for downstream valorization. This approach also introduces new chemical functionalities, leading to what is called "technical lignin" (Kropat et al., 2021). As a result, most of the lignin is burned onsite for energy generation. Lignin-first biorefinery is an emerging biomass valorization approach that prioritizes the selective extraction and stabilization of lignin at the start of biomass fractionation processes (Luo et al., 2023).

In the context of lignin first biorefinery, obtaining “native like lignin” is crucial for its full potential valorization. This preserves the structural features, in particular the β -O-4 linkage. These are the most amenable bonds to depolymerize lignin into high-value aromatic monomers. Thus, the development of methods that enable the extraction of lignin close to its native structure are paramount importance (Wang and Deuss, 2023).

One of the most studied strategies is reductive catalytic fractionation (RCF), which involves fractionating lignocellulosic biomass using an alcohol solvent (e.g., methanol, ethanol) and a metal-based hydrogenation catalyst (Pd/C, Ru/C) under a reducing atmosphere. This method results in the preservation of high β -O-4 bonds by stabilizing reactive intermediates during solvolysis. The phenolic monomers obtained from this kind of lignin show low condensation tendency (Liao et al., 2020; Luo et al., 2023). Other authors use protective chemistry to stabilize reactive lignin intermediates with aldehydes or polyols. In this approach, acetals or ethers are formed during fractionation, thereby preventing recondensation and enabling recovery of native-like lignin with β -O-4 linkages intact (Cheng et al., 2024; Wang and Deuss, 2023). Recently, deep eutectic solvents (DESs) have gained prominence as green solvents for lignin-first extraction. For example, (He et al., 2025) demonstrated that TMAH-based alkaline DESs can achieve delignification rates above 67% at 50°C while preserving up to 88% β -O-4 linkages from coconut shell lignin. Moreover, pyridine hydrochloride-based DES systems showed preservation of 42.1 β -O-4 units per 100 aromatic units under mild conditions (Wang et al., 2025).

The advantages of lignin first biorefineries is their approach to retain the integrity of not only lignin but also cellulose and hemicellulose. Wang et al. (2025) demonstrated that a pyridine hydrochloride-based DES system resulted a cellulose rich residue which achieved an enzymatic glucose yield of 88.2% while also preserving β -O-4 linkages. Similarly, Cheng et al. (2024)

reported that lignin-first fractionation of biomass with DES enabled the co-production of high-quality fermentable sugars and lignin-based adhesives. In another study, Liao et al. (2024) demonstrated a sustainable biorefinery framework where lignin was selectively extracted and depolymerized into phenolic monomers while the residual carbohydrates were effectively hydrolyzed into glucose and xylose with high saccharification efficiency. These findings showcase the synergistic potential of lignin-first systems to generate both aromatic chemicals from lignin and sugar-derived products such as bioethanol, furans, and organic acids from the carbohydrate fraction.

Several companies and startups exist that are pioneering lignin-first biorefinery technologies. Foreexample, Fibenol (Estonia) focuses on fractionating hardwood biomass to produce high-purity lignin, sugars, and specialty chemicals using their proprietary Sunburst™ pretreatment technology that uses heat, pressure and mechanical power to turn wood chips into a chocolate mousse-like slurry that can then be converted into biomaterials. LXP Group (Germany) uses a patented Lignin Extraction Process (LXP) to selectively isolate native lignin while preserving carbohydrate fractions for further valorization. Attis Innovations (USA) is building integrated biorefineries that convert the lignin into performance materials and biofuels.

Despite the promising potential of lignin-first biorefineries, there exist technical and economic challenges that hinder their industrial advancement. One such challenge is the difficulty of simultaneously preserving the quality of all lignocellulosic components (Renders et al., 2017). When catalytic systems are employed for biomass fractionation, catalyst recovery is non-trivial. The stability of lignin-derived intermediates also presents a bottleneck in lignin-first circular biorefinery (Abu-Omar et al., 2021; Luo et al., 2020). The natural heterogeneity of lignin and the batch to batch variability across different feedstocks (e.g., varying S/G ratios, β -O-4 content) also affects both the extraction and monomer yields, which makes standardized processing difficult. Genetic engineering of plants to produce more depolymerizable lignin (e.g., via higher S-content or ester-linked monolignols) shows promise although it raises issues with plant fitness, growth, or cell wall integrity ((Ralph et al., 2019). Techno-economic assessments also reveal that lignin-first biorefineries may require more complex operations, and additional reagents, to compete with conventional biomass processing (Liao et al., 2020). Addressing these challenges is crucial for realizing the full potential of lignin-first biorefineries. The use of deep eutectic solvents to fractionate biomass can overcome some of the aforementioned challenges and is reviewed in detail in the subsequent chapters.

2.3. Methods of biomass fractionation

Effective fractionation of lignocellulosic biomass is critical for converting its structural components (cellulose, hemicellulose, and lignin) into high-value products. Over the years,

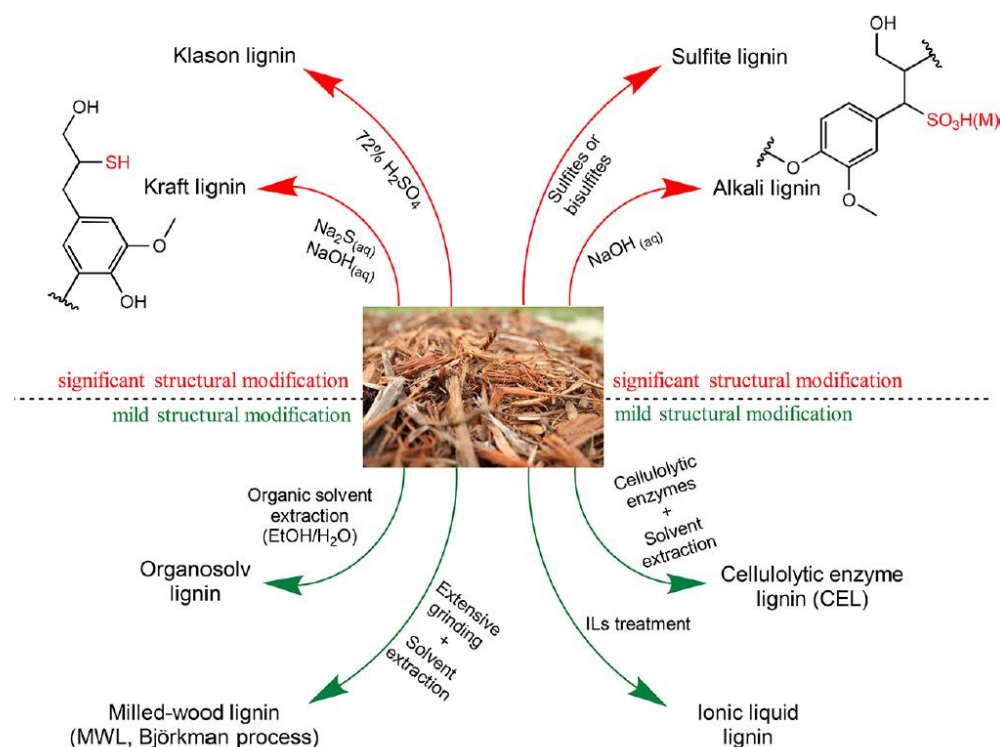


Figure 5: different methods for isolating lignin from lignocellulosic biomass adopted from (Sun et al., 2018)

several physical, chemical, and physicochemical pretreatment strategies have been developed (see Figure 5). Among the most industrialized are alkaline and acid hydrolysis methods, notably the kraft and sulfite processes, which solubilize lignin to recover cellulose but they severely alter lignin's structure (Lobato-Peralta et al., 2021; Rodrigues et al., 2021). Organosolv pretreatment has emerged as a cleaner, sulfur-free alternative, using organic solvents (e.g., ethanol, acetone). Organosolv pretreatment yields purer lignin with partially preserved β -O-4 linkages, although solvent recovery and flammability remain concerns (Arni, 2018). Ionic liquids (ILs) have also been used to fractionate biomass due to their tunability and ability to solubilize lignin without harsh conditions. However, their high cost and recyclability challenges hinder scale-up (Bertella and Luterbacher, 2020). Biological methods involving fungi or bacterial are good alternatives in terms of energy requirements but take longer time and are hard to control (Arni, 2018).

2.3.1. Biomass fractionation with deep eutectic solvents

2.3.1.1. Deep eutectic solvents

Deep eutectic solvents (DES) are solvents possessing a lower melting point than their pure components. They are eutectic mixtures of hydrogen bond donors (HBDs) and hydrogen bond acceptors (HBAs) (Chen et al., 2020b). They are an emerging class of liquids that gained increased attention in the past two decades after Abbott et al. noticed a decrease in the melting

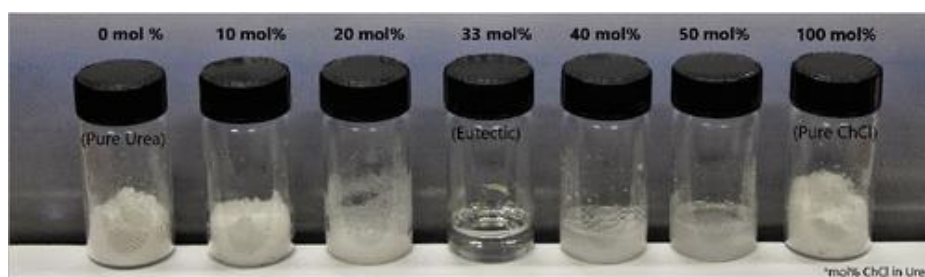
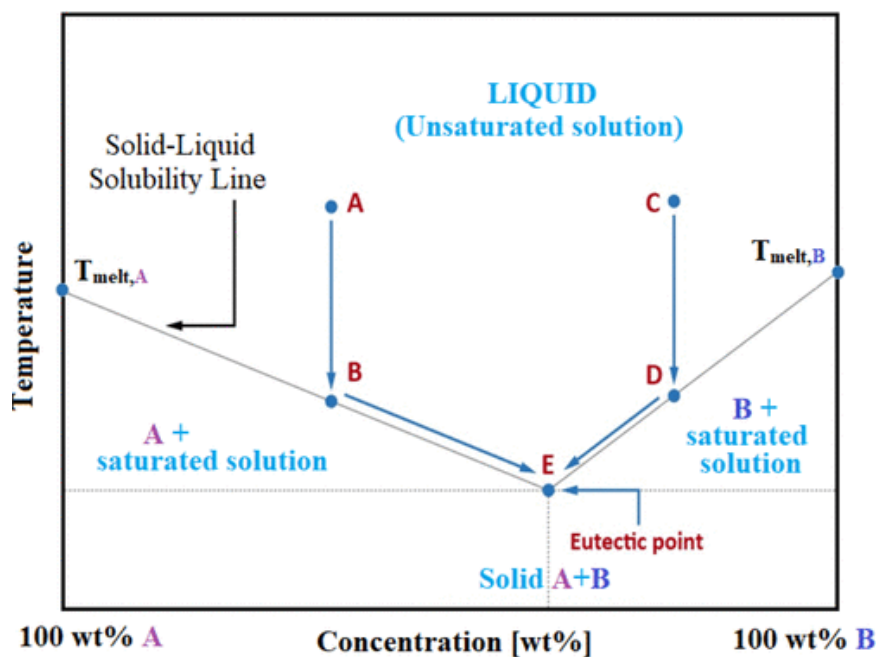


Figure 6: I) binary phase diagram for eutectic mixtures II) Phase change for Choline chloride/urea as a function of mole fraction

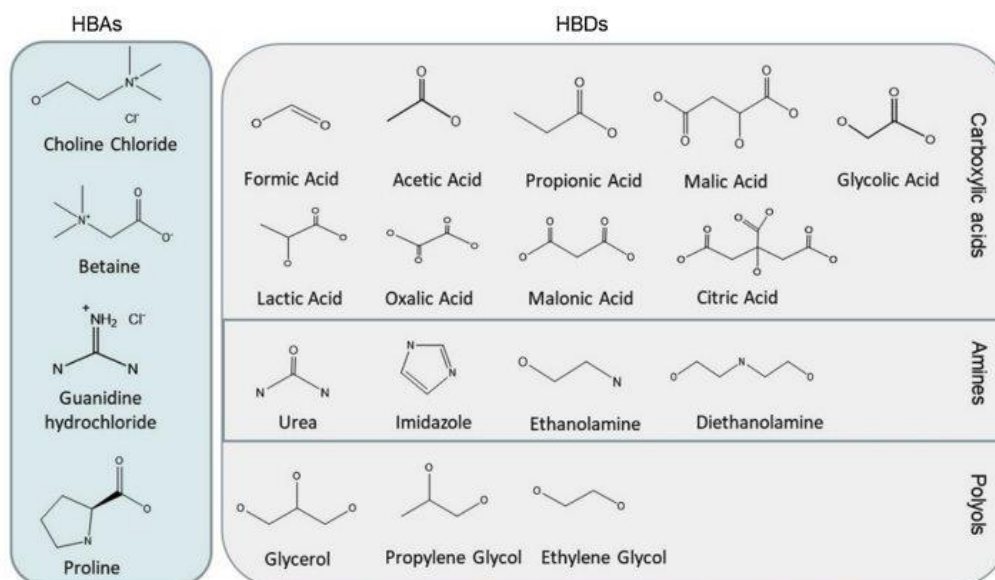


Figure 7: Combinations of hydrogen bond acceptors (HBAs) and hydrogen bond donors (HBDs) (Chen et al., 2020b)

point of certain mixtures of hydrogen bond donors (HBDs) and hydrogen bond acceptors (HBAs) (Hansen et al., 2021). Notice in Figure 6II how the phase of a choline chloride and urea mixture changes as a function of mole fraction of the components. Figure 7 also shows different combinations of HBAs and HBDs for DES preparation

The preparation of DESs is usually easy. It involves heating and stirring the constituents together under an inert atmosphere to obtain a homogeneous and clear liquid. During Des preparation, no additional reactions are envisioned to occur. Their preparation is interesting in that no additional solvent is required and no subsequent purification step is required making them a viable solvent for biomass fractionation (Hansen et al., 2021). This simplicity means low production costs. DESs are estimated to cost as little as 20% of typical ionic liquids (Lobato-Rodríguez et al., 2023). In addition to their easy synthesis, DESs exhibit favorable features like low vapor pressure, biodegradability, and low toxicity (Alonso et al., 2016). Furthermore, the physico-chemical properties of DESs can be tailored by adjusting HBA/HBD combinations and ratios to optimize delignification efficiency and structural preservation (Provost et al., 2022).

Based on the chemical nature of their HBDs and HBAs, DESs are classified into five types. Type I DESs consist of a quaternary ammonium salt (typically choline chloride) and a metal chloride such as $ZnCl_2$ and $AlCl_3$. The resulting system is capable of coordinating with various anions through ionic interactions. Type II DESs are similar but use hydrated metal chlorides, which leads to more complex hydrogen bonding networks. Type III DESs involve a quaternary ammonium salt as the HBA and a neutral organic molecule such as a polyol (glycerol, ethylene glycol etc), carboxylic acid, or amide as the HBD. Type IV DESs combine a metal chloride hydrate as the HBA with an organic HBD. They create systems with both ionic and molecular characteristics and are often used in metal processing. Type V DESs are the newest class and are composed entirely of non-ionic molecular components (e.g., thymol with lactic acid or menthol with fatty acids). Type III DESs are the most used especially in biomass fractionation due to their ease of synthesis and low toxicity (Hansen et al., 2021).

Factors influencing Lignin extraction during DES-Based fractionation

Type and nature of DES

The acidity, basicity, or neutrality of deep eutectic solvents (DESs) plays a decisive role in determining lignin extraction efficiency, yield, purity, and structural integrity. Acidic DESs, which typically consist of choline chloride as HBA and a variety of organic acids (e.g., lactic acid, oxalic acid, malonic acid) as HBD, effectively cleave ether bonds and ester linkages in lignin and lignin-carbohydrate complexes through proton-catalyzed mechanisms (Chen et al., 2020b). Several researchers have studied the delignification ability of acidic DESs. For example, ChCl:oxalic acid (1:1) achieved 98.5% delignification from corncob at 90°C for 24 h, while ChCl:lactic acid (1:15) reached 93.1% under the same conditions (Chen et al., 2020b). Xiao et al., (2024) further noted that acidic DESs enable the isolation of low molecular weight and structurally uniform lignin. It is important to optimize acidic DESs as too much acidity may lead to condensation of lignin and distraction of β -O-4 linkages. For Example, (Z. Chen et al., 2020) extracted lignin from Switchgras with ChCL/Ethylene glycol (EG) (1:2;n/n) at 110°C,

20w% H₂O and different concentrations of H₂SO₄ (0.5w% and 1w%). They found that 40.3% and 24.4% β -O-4 bond were retained respectively when 0.5w% and 1w% of H₂SO₄ was used.

Basic DESs on the other hand dissolve lignin via deprotonation of phenolic hydroxyls. These solvents are less aggressive than acidic ones. For example, a DES composed of ChCl and monoethanolamine (MEA) (1:6) removed 81% lignin from wheat straw at 90°C in 12h (Jose et al., 2023). Basic DESs extracted lignin tend to have preserved functional groups and lower condensation levels, which are advantageous for downstream valorization like depolymerization. However, basic DESs generally require higher temperatures or longer durations to reach yields comparable to acidic systems.

Neutral DESs are also studied for lignin extraction. They are often based on polyols like glycerol or ethylene glycol and exhibit moderate delignification ability. For example, ChCl:glycerol (1:2) removed 71.3% lignin from corncob at 90°C in 24h (Jose et al., 2023). Compared to acidic DES, neutral DESs are less efficient but they preserve the structural integrity of lignin and exhibit good biocompatibility. Among neutral DESs, DESs having less hydroxyl groups in the HBD (ethylene glycol) outperform those having many hydroxyl groups (glycerol or xylitol) due to reduced hydrogen bonding within the solvent, which improves lignin accessibility (Hong et al., 2020b).

Another parameter affecting delignification efficiency and lignin structure is the molar ratio of DES components. In a study by Chen et al. (2020) using choline chloride (ChCl) and ethylene glycol (EG), the authors demonstrated that increasing the ChCl:EG molar ratio from 1:2 to 3:2 increased the abundance of β -O-4 linkages in the extracted lignin from 24.4% to 31.0% under same extraction conditions (110 °C, 1.0 wt% H₂SO₄). They attributed this preservation of bonds to the higher concentration of chloride ions (Cl⁻), which stabilize the benzylic carbocation intermediate formed during β -O-4 bond cleavage, thus preventing condensation reactions (Chen et al., 2020a).

Extraction temperature

Temperature is a critical factor during lignin extraction. It affects yield and structural preservation. Generally, increasing temperature improves lignin yield up to an optimal point. Zhang et al. (2022) reported that increasing extraction temperature from 100 °C to 150 °C raised lignin recovery from 41.3% to 95.9% when extracting lignin from corncob using ChCl:lactic acid. Zhang et al. (2023) observed that lignin yield from pine using an AlCl₃-based DES peaked at 91.1 ± 2.6% at 120 °C, but declined sharply to 41.9 ± 2.7% at 150 °C due to increased condensation that reduced lignin solubility. The reader is advised to look at Table-3 for more information on the effect of extraction conditions including temperature.

Temperature also influences lignin purity by facilitating carbohydrate removal. Chen et al. (2020) showed that lignin purity improved from 78.7% to 91.4% as temperature increased from 110 °C to 130 °C in ChCl:EG systems, but slightly declined at 150 °C due to increased formation of side products such as pseudo lignin and EG adducts. High temperatures also tends to result in lignin with uniform fractions. Lignin treated at ≥110 °C with ternary DESs showed reduced molecular weight distribution, which can be beneficial for nanoparticle self-assembly (Liu et al., 2019).

It is worth mentioning that although high temperatures result in increased yield, they promote cleavage of β -O-4 linkages. Excessive temperature increases recalcitrant C–C bonds thereby reducing monomer yield during depolymerization. Hong et al. (2020) reported a 69% reduction in β -O-4 content when temperature increased from 80 °C to 130 °C during ChCl:LA pretreatment. Rodrigues et al. (2024) recommended limiting temperatures to below 120 °C to preserve the aryl-ether structure and maintain lignin reactivity for downstream applications.

Extraction time

Time is another factor that influences extraction yield, purity, and lignin structure in DES mediated biomass fractionation. Prolonged time allows better dissolution of lignin in the solvent which results in enhanced lignin yield. More and more lignin-carbohydrate linkages and solubilization of lignin fragments happen with time. However, time doesn't indefinitely improve yield. For example, Rodrigues et al., (2024) observed that optimal lignin extraction (yield = $90.08 \pm 1.42\%$) occurred at 123 °C for 6 h ours. They argued that further increasing time did not significantly increase the yield.

The role of extraction time during lignin extraction is less pronounced than that of temperature. Zhang et al., (2022) investigated the extraction of lignin from corncob residue using ChCl/LA (1:10; molar) with varying temperature (100°C, 120°C, 150°C) and time (6h, 12h, and 18h). Their yield varied between 41.3% to 85.6% and they argued that the variation was mainly driven by temperature, not time. Their statistical analysis revealed that temperature had a significant positive correlation ($P < 0.05$) with yield, whereas time had no statistically significant impact under fixed temperature. The purity also peaked at 97.8% under these at 150°C and 6h, while varying time from 6 to 18 hours showed negligible impact.

Extraction time can affect the molecular integrity of DES-extracted lignin. (Lou and Zhang, 2022) studied the effect of a two-stage pretreatment (presoaking in DES at room temperature followed by extraction) on wheat straw. They found that increasing presoaking time reduced the number-average and weight-average molecular weights (M_n and M_w), indicating progressive lignin depolymerization. Wheat straw subjected to 3h and 24 h DES presoaking exhibited M_w and values of 800–1200 g/mol and 1700–2000 g/mol respectively.

Although extended times may enhance extraction, longer durations can lead to over-degradation, condensation, or formation of undesired pseudolignin. Therefore, for optimal valorization, particularly in selective bond cleavage pathways, moderate extraction times (3–6 h) appear effective.

Table 3: Extraction conditions, yield and purity of different DESs

DES (molar ratio)	Biomass	Temp (°C)	Time (h)	Lignin Yield (%)	Purity (%)	Reference
ChCl:LA (1:2)	Corn cob	90	24	64.7	-	(Zhang et al., 2016)
ChCl:LA (1:10)	Corn cob	150	18.0	85.6	97.8	(Zhang et al., 2022)
ChCl:LA (1:15)	Corn cob	90	24	93.1	-	(Zhang et al., 2016)

K ₂ CO ₃ :Gly (1:5)	Wheat straw	100	16.0	7.8	60.1	(Yue et al., 2022)
ChCl:LA (1:5)	Eucalyptus	110	6.0	80.0	-	(Shen et al., 2019)
ChCl:OA (1:1)	Corncob	90	24.0	98.5	-	(Zhang et al., 2016)
ChCl:Gly (1:2)	Corncob	150	15.0	59.0	-	(Procentese et al., 2015)
ChCl:LA (1:10)	Willow	120	12.0	-	High	(Lyu et al., 2018)
ChCl:LA (1:2)	Poplar	145	6.0	-	95	(Alvarez-Vasco et al., 2016)
ChCl:Gly (1:2)	Switchgrass	120	1.0	76.6	-	(Chen et al., 2020b)
ChCl:EG (1:2)	Switchgrass	130	0.5	87.0	-	(Chen et al., 2020b)
GH:EG:PTSA (1:1.94:0.06)	Switchgrass	120	0.1	82.0	-	(Chen et al., 2020b)
ChCl :LA (1 :2)	Cornstover	130	2	80.3		(Liang et al., 2021)

2.3.2. Tailoring lignin properties through solvatochromic tuning of deep eutectic solvents

Tuning the composition of DES influences lignin structure post-extraction as discussed in section (insert section). The structure of extracted lignin influences the efficiency of downstream valorization pathways. By carefully selecting DES components, it is possible to alter the molecular weight, functional group content, β -O-4 linkage content, and reactivity of lignin. Tailoring the properties of DES extracted lignin can be approached by different strategies. Traditionally, the design of effective DESs has relied on empirical screening, based on trial-and-error combinations HBAs and HBDs. This trial-and-error approach is time-consuming and lacks predictive power. Recently, more predictive strategies like quantum chemical calculations, molecular dynamics simulations, and solvatochromic analysis has emerged (Xiao et al., 2024).

Kamlet-Taft parameters are discussed in detail in this section. They are based on solvatochromic and characterizes DESs using three parameters:

- α (hydrogen bond donating ability)
- β (hydrogen bond accepting ability)
- π^* (dipolarity/polarizability)

These parameters were originally introduced by Kamlet and Taft in the 1970s to quantify solvent effects on chemical processes through linear solvation energy relationships (LSERs) (Dwamena and Raynie, 2020). The α parameter reflects a solvent's capacity to donate hydrogen bonds to solutes, which is critical in proton transfer and bond cleavage processes. The β parameter quantifies the solvent's ability to accept hydrogen bonds. π describes the solvent's polarity and polarizability meaning the ability to capture non-specific dipole-dipole and dispersion interactions that influence solute solvation (Zhang et al., 2023a).

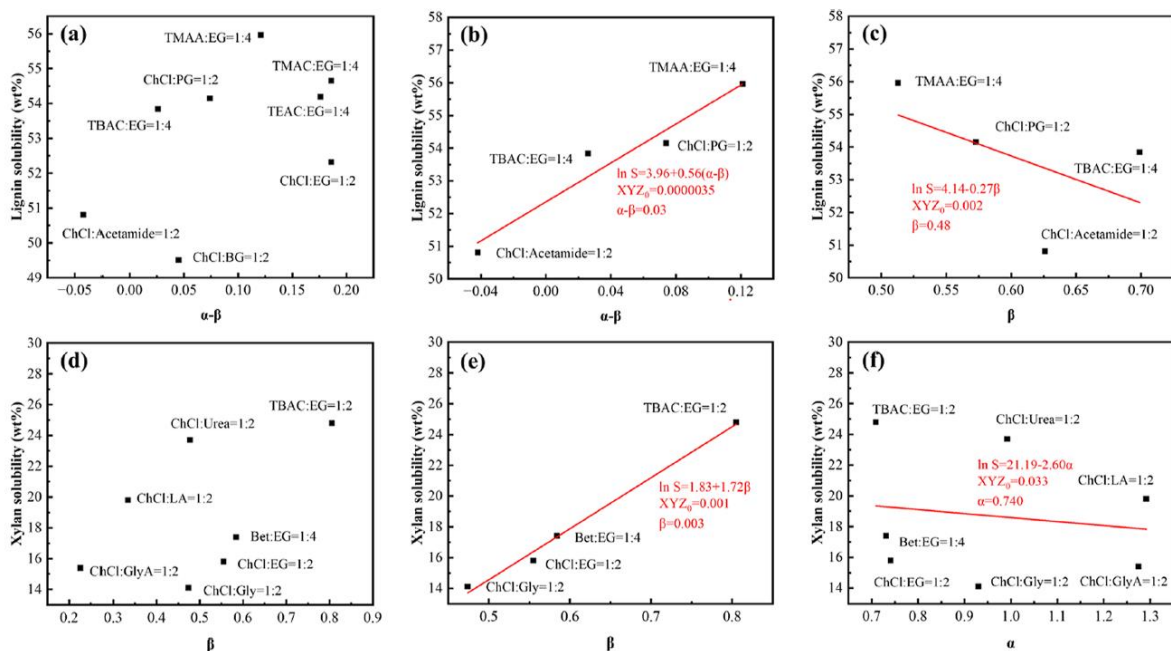


Figure 8: Kamlet-Taft parameters of different DESs and their relationship with lignin solubility (a-c) and xylan solubility (d-f) adopted from (Zhang et al., 2023a)

These parameters are tunable in DES systems by changing the composition of HBA/HBD. Studies have shown that increasing the acidity (α) of a DES typically enhances lignin dissolution. Liang et al. (2021) reported a linear relationship between DES acidity (α) and delignification performance ($R^2 = 0.75$). Zhang et al. (2023) extended this observation across 56 DES systems, showing that lignin solubility increased with both α and π^* , but not with β . More specifically, lignin dissolution correlated better with the combined net acidity term ($\alpha - \beta$), suggesting that high HBD strength coupled with low basicity favors lignin dissolution. Conversely, the β parameter plays a dominant role in hemicellulose and cellulose dissolution. Zhang et al. (2023) observed a positive linear relationship between β values and xylan solubility (Figure 8). This is attributed to the ability of basic DESs to accept hydrogen bonds from hydroxyl-rich

polysaccharides, which facilitates disruption of their intermolecular networks. For cellulose, a combination of high β and an optimal net basicity ($\beta - \alpha$ between 0.35 and 0.90) is critical for dissolution. The π^* parameter also contributes to lignin solubility by stabilizing polar intermediates and enhancing the interaction with aromatic rings. Its effect, however, is weaker and less predictable than α (Zhang et al., 2023a).

The Kamlet-Taft parameters also give insight into lignin's structure, functional group profile, and molecular weight. A tradeoff between lignin yield and preserving its structure is usually observed. High solvent acidity ($\alpha > 1.2$), as found in DESs like ChCl:formic acid or ChCl:gallic acid, facilitates efficient lignin solubilization but also cleave β -O-4 linkages via acidolysis (Zhang et al., 2023a). Liang et al., (2021) also noted a decline in β -O-4 content under highly acidic conditions. Moderating the acidity with cosolvents like ethanol has been found to stabilize β -O-4 linkages. A study involving ChCl:citric acid DES with and without ethanol

demonstrated that up to 40.3% β -O-4 linkage were retained in the presence of ethanol which was five times higher than the DES alone (Li et al., 2024). Besides, Lignin reactivity depends on accessible functional groups, notably phenolic and carboxylic moieties. The net acidity (α - β) was found to correlate positively with phenolic OH enrichment in lignin extracted from organosolv and enzymatic hydrolysis (Liu et al., 2019).

2.4. Lignin depolymerization

The use of extracted lignin as is for high value applications is limited. Unlocking its full potential requires downstream valorization. That is where depolymerization comes into play to transform lignin into lower molecular weight aromatic compounds that can serve as precursors for the production of fuels, resins, or fine chemicals. Due to lignin's structural irregularity, a selective and controllable depolymerization process remains a challenge.

Cleavage of β -O-4 bonds is the primary target of many depolymerization strategies, given its abundance and relative lability compared to C-C bonds (Wang et al., 2013).

The bond cleavage involves mechanisms like acidolysis, hydrolysis, hydrogenolysis, and oxidation. In acid or base catalyzed processes, hydrolytic cleavage is typically initiated via protonation (acidic) or nucleophilic attack (basic) at the α -position thereby cleaving the ether bond and subsequent formation of phenolic monomers. In contrast, oxidative pathways target electron rich aromatic centers or side chains to generate quinones and carboxylated aromatic compounds. These mechanisms can proceed via metal-oxo species, peroxides, or oxygen radicals and are often highly selective depending on the catalyst and reaction conditions (Roy et al., 2022). In contrast, reductive depolymerization mechanisms such as hydrogenolysis use transition metal catalysts (Ru/C, Pd/C) to break C-O and even C-C bonds under hydrogen atmosphere (Wang et al., 2013).

2.4.1. Thermal depolymerization

Thermal depolymerization also known as pyrolysis involves treating lignin between 300 and 600 °C under inert conditions. Pyrolysis breaks down lignin through homolytic and heterolytic cleavage of key linkages (β -O-4, β -5, 5-5'). This results in the formation of phenolic monomers such as guaiacol, syringol, and catechol derivatives. As an example, pyrolysis of kraft lignin at 500 °C yielded up to 35% bio-oil containing phenolics. Char and light gases like CO, CO₂, CH₄, and H₂ were also produced (Chio et al., 2019). Pyrolysis suffers from low selectivity due to extensive secondary reactions such as recondensation and repolymerization. The yield and quality of products are sensitive to process parameters. Fast pyrolysis is characterized by rapid heating and short residence times, tends to favor bio-oil production, whereas slow pyrolysis results in more solid residue. For example, studies report that fast pyrolysis of organosolv lignin at 500 °C can achieve bio-oil yields as high as 45% by weight compared to less than 30% for slow pyrolysis under the same temperature (Wang et al., 2013).

2.4.2. Chemical depolymerization

This method involves the use of acid or base to cleave ether linkages in lignin. In acid-catalyzed systems, the acid promotes cleavage of ether bonds via protonation of the oxygen atom, followed by carbocation formation and bond scission. This method works effectively at moderate temperatures (120–250 °C). Base-catalyzed depolymerization (BCD) happens

through nucleophilic attack on lignin's ether bonds at elevated temperatures (200–300 °C)(Chio et al., 2019).

2.4.3. Reductive and oxidative depolymerization

Reductive depolymerization of lignin uses hydrogen in the presence of metal catalysts (Pd, Ni, Ru, Cu). In this method, reactive intermediates formed during bond cleavage are stabilized by hydrogen. This strategy minimizes undesired condensation reactions thereby maximizing monomer yields. In contrast, oxidative depolymerization uses oxygen or peroxides, often in the presence of metal catalysts (Cu, Mn, Pd). This approach yields highly functionalized aromatic aldehydes or acids. Vanillin and syringaldehyde are among the most frequently reported products (Bourbiaux et al., 2021).

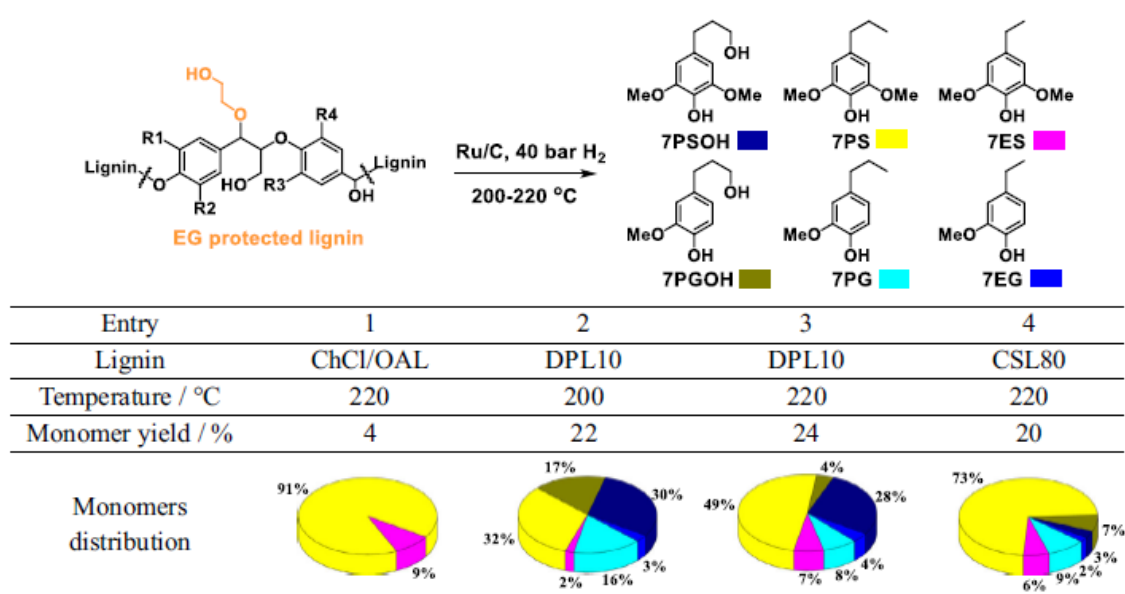


Figure 9: Depolymerization of DES-extracted lignin by hydrogenolysis ; depolymerization conditions (200 mg DES fractionated lignin, 200 mg Ru/C (5 wt% Ru loading), 20mL methanol, 18 h); Abbreviations : DPL= Derivatization protection Lignin (extracted by Derivatization protection DES =ChCl/EG/OA), CSL = cleavage stabilization Lignin (extracted by cleavage stabilization DES= ChCl/OA); the numbers in DPL10 and CSL80 refers to %w of OA and EG in the ternary DES respectively.

Figure 9 shows a study by (Liu et al., 2021) where they depolymerized DES extracted lignin by hydrogenolysis. The hydrogenolysis was carried out using Ru/C at 40 bar H₂ and 200–220 °C. The oxalic acid containing ternary DES (DPDES10 = ChCl/EG/oxalic acid; 1:2:10%w) extracted lignin (DPL10) showed the highest monomer yields of 22% at 200 °C and 24% at 220 °C. The enhanced yields for this particular DES was attributed to better preservation of β-O-4 structures due to EG protection during fractionation.

2.4.4. Biological depolymerization

Biological depolymerization employs microorganisms and enzymes that degrade lignin. The key enzymes involved include lignin peroxidase (LiP), manganese peroxidase (MnP), and laccases. Biological depolymerization cleaves ether bonds in lignin under ambient conditions. In addition to being environmentally benign, they offer high specificity. Their main limitations are slow reaction rates, and sensitivity of enzymes to lignin heterogeneity. Enzyme inactivation, substrate accessibility, and the tendency of microorganisms to prefer simpler carbon sources also hinder efficiency (Xu et al., 2018).

2.4.5. Electrochemical depolymerization

Electrochemical depolymerization (ECD) of lignin is a recent and attractive approach for lignin valorization. Unlike thermal or chemical methods, it requires mild reaction conditions and no reagents. Renewable energy sources such as wind and solar can be used during electrochemical depolymerization making the process more sustainable (Garedew et al., 2021).

The process can proceed through either oxidative or reductive pathways. In oxidative depolymerization, lignin is degraded by electron transfer from its phenolic or benzylic groups to the anode, facilitating cleavage of C–O and C–C bonds. However, oxidative pathways are prone to overoxidation, producing low-value carboxylic acids and CO₂ if the reaction isn't properly controlled. Stiefel et al., (2015) addressed the problem of overoxidation by designing an electrochemical membrane that integrates nanofiltration as depicted in Figure 10. In their setup, depolymerized low-molecular-weight lignin products are continuously removed from the oxidative environment via a ceramic membrane. Reductive electrochemical depolymerization occurs in the cathode to reduce oxygenated functional groups. The cathodic reaction enhances the yield of reduced aromatics (Alves da Cruz et al., 2022).

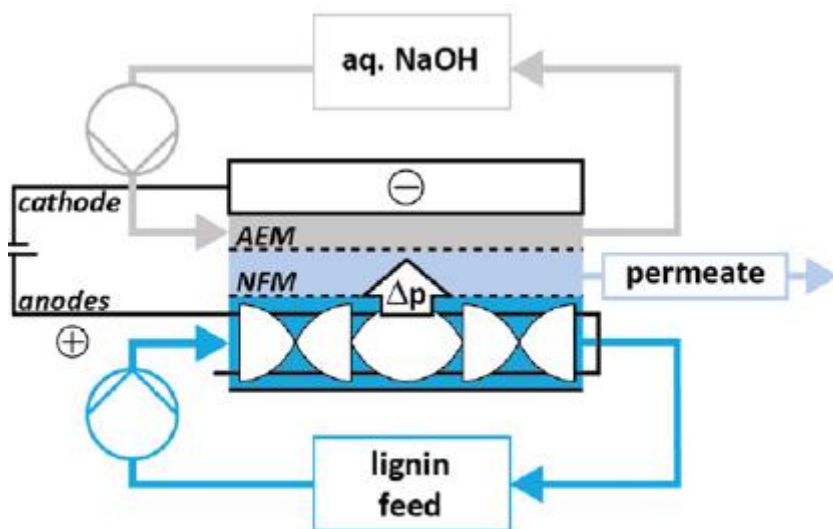


Figure 10: Schematic of electrochemical membrane (AEM: Anion Exchange Membrane, NFM: Nanofiltration Membrane) (Stiefel et al., 2015)

It is important to mention that the choice of electrode materials is critical during electrochemical depolymerization of lignin. Noble metals like Pt and Ru can be highly active but are costly and prone to competitive hydrogen evolution. In contrast, cheaper metals like Cu and Ni show

moderate activity but better selectivity (Ayub and Raheel, 2022). The solvent also affects the degree of depolymerization by influencing the solubility and reactivity of lignin in the electrochemical system. Aqueous alkaline media have been widely used. Recently newer solvents are being employed. Alves da Cruz et al., (2022) employed Levulinic acid, which itself is formed during the hydrothermal processing of lignocellulosic biomass, to dissolve lignin during electrochemical depolymerization giving insights into greener approaches. Their system achieved good solubility and 5-15 wt% yields of monomers like 4-propylguaiacol and 4-propylsyringol from hardwood lignin using a simple Cu cathode. γ -Valerolactone, and ionic liquids have also been studied as solvents during electrochemical depolymerization (Garedew et al., 2021).

In spite of its greener nature, electrochemical depolymerization faces challenges. One such challenge is low current efficiency. Additionally, electrode fouling by lignin or its depolymerized fragments can decrease activity over time. In oxidative setups, there's a high risk of overoxidation as discussed previously. Moreover, the structural complexity and heterogeneity of technical lignin makes it difficult to achieve uniform reactivity or predict product profiles but this is mostly common for all methods (Ayub and Raheel, 2022).

3 Materials and Methods

This project was performed at the laboratory of Hubert Curien Multidisciplinary Institute (IPHC-UMR 7178, CNRS) located in Strasbourg, France. The IPHC is a renowned research laboratory located in Strasbourg, under the joint supervision of the Centre national de la recherche scientifique (CNRS) and the University of Strasbourg. This institute is distinguished by its multidisciplinary nature, bringing together diverse expertise in the fields of physics, chemistry, and biology to address major societal challenges. This project was done in a team working in molecular recognition and separation processes (RePSeM) supervised by Professor B. Ernst.

3.1. Materials

Brewery spent grain (BSG) is the biomass studied in this project, and it was acquired by the RePSEM team from nearby sources.

3.2. Methods

3.2.1. Biomass pretreatment

3.2.1.1. Soxhlet extraction

The raw brewery spent grain was first crushed to sizes below 0.5mm using a pilot-scale disc mill. Prior to its use in lignin extraction, the brewery spent grain was pretreated to remove impurities. These impurities may interfere with the extraction process affecting yield and purity. Soxhlet extractor (Figure 11) was employed to remove polyphenols, free sugars, and proteins. For this, the biomass was first dried at 60°C overnight. Approximately 5 g of dried biomass was weighed and placed into a cellulose extraction cartridge, which was loaded into the Soxhlet extractor. The extractables were removed in a sequential manner in which the biomass was treated with hexane, ethanol, and distilled water respectively at their respective boiling temperatures. The extraction with hexane was to target fatty acids using 200 mL of hexane in a 250 mL round-bottom flask. The system was assembled as in Figure 11, and extraction conducted at 69°C under reflux for 6 hours. After completion, the hexane extract was removed and replaced with another 250 mL flask filled with 200 mL of ethanol to remove polyphenols. After another 6 hours at 79°C, the flask containing ethanol was replaced with another similar flask filled with 200 mL of osmosis water to extract proteins and free sugars at 100°C under reflux for 6 hours. The flask and the cellulose cartridge were then removed from the Soxhlet apparatus. The treated biomass was carefully collected with a spatula and transferred to an aluminum dish. The biomass was then dried at 60°C for 12–24 hours until a constant mass was obtained, after which the final weight was recorded. The mass of extractives per oven dry weight (ODW) was determined (equation 1- 3).

$$\%total\ solids = \frac{(Weight_{crucible\ plus\ dry\ sample} - Weight_{crucible}) * 100}{(Weight_{crucible\ plus\ sample} - Weight_{crucible})} \quad (1)$$

$$ODW = \frac{(Weight_{crucible \text{ plus sample}} - Weight_{crucible}) * \% \text{ total solids}}{100} \quad (2)$$

$$\%Extractives = \frac{(Weight_{flask \text{ plus extractives}} - Weight_{flask}) * 100}{ODW} \quad (3)$$

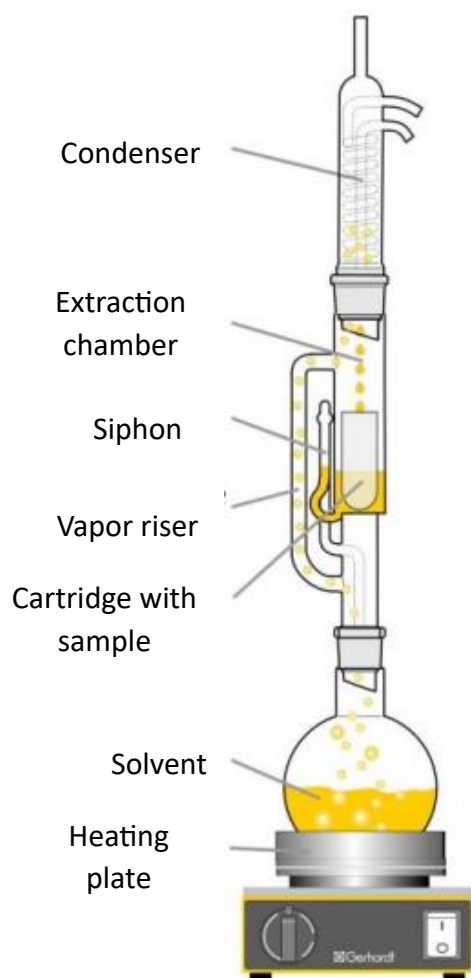


Figure 11: Schematic of a soxhlet extractor

To know the amount of extractables extracted in each stage of the Soxhlet extraction, the solvents were removed in rotavapor under vacuum. The flasks were further dried in an oven at 60°C and then weighed and equations (1-3) were used on each stage of extraction and the results are given in Table 3.

Table 3: % of extractables (g/g) removed in each stage of Soxhlet extraction

Soxhlet Extraction step	Hexane	Ethanol	Distilled water
% Extractables removed	5.1 ± 0.8	7.7 ± 0.3	16.86 ± 2.3

3.2.1.2. Hydrothermal treatment

Brewery spent grain has high protein content. According to (Provost et al., 2022), it contains 24.9 ± 1.60 g/100g dry weight of proteins. Our CHN elemental analysis shows that it contains 18.7% of proteins (see section 3.2.8). Soxhlet extraction alone may not be enough to remove all the proteins. The Soxhlet pretreated biomass was further treated hydrothermally. This was done by mixing 4% (mass/volume) of the biomass with distilled water and keep it at 60°C under stirring for 24 hours.

3.2.2. DES preparation

Fresh deep eutectic solvents were synthesized prior to each extraction (the latest preparation was done the evening before the extraction day). Three types of DES were studied in this work. A DES composed of choline chloride and lactic acid (ChCl/LA) had been prepared in 1:1 and 1:10 molar ratios. The third DES studied was a ternary DES composed of ChCl and ethylene glycol (EG) in 1:2 molar ratio and containing 10% w/w of oxalic acid (OA). The quantities of each component were calculated using equation (4). The DES was prepared by mixing the components and heating the mixtures between 60- 70°C under magnetic stirring at 500 rpm until a clear liquid was obtained. The prepared DES was stored in a desiccator until it was used. For a DES composed of i and j components with molar ratio n:m, the mass of each component is calculated as follows:

$$mass\ component_i = \frac{MW_i * n}{(MW_i * n + MW_j * m) * purity} * total\ mass\ of\ DES \quad (4)$$

Table 4: Quantities of pure components required to prepare 100 g of DES

DES molar ratio	Components (g)			
	ChCl (HBA, Tm* = 302 °C)	LA (HBD, Tm = 17 °C)	EG (HBD, Tm = -12.9 °C)	OA (HBD, Tm = 189 °C)
ChCl/LA (1:1)	60.79	39.21	-	-
ChCl/LA (1:10)	13.42	86.58	-	-
ChCl/EG/OA (1:2:10%w)	48.16	-	42.80	9.04

* Tm is the melting temperature of compound, HBA = hydrogen bond acceptor, HBD = hydrogen bond donor,

3.2.3. Extraction

Before starting extraction, glass microfiber filters (2.7 µm, 90 mm) were placed in aluminum plates and dried in an oven at 60 °C for at least 4 hours and subsequently transferred to a desiccator for 30 minutes before weighing. These pre-weighed filters were used for filtering the extract. Moreover, a washing solution consisting of ethanol and deionized water (1:9, v/v) was prepared to be used later to remove residual hemicelluloses and DES from lignin.

Figure 12a schematically presents the extraction with ChCl/LA DESs. The extraction was performed by mixing the brewery spent grain and DES in a 1:20 (m/m) ratio. The mixture was heated in an oil bath (placed in heating plate) which was maintained at the target extraction temperature (100 or 140°C) for 3 hours. A magnetic stirrer ensured continuous agitation at 500 rpm. Once the extraction was complete, the mixture was cooled to room temperature under a fume hood. 60 mL of ethanol was added for 2 g of biomass to quench the reaction and magnetically stirred for 30 minutes at room temperature. The mixture was filtered using a Büchner funnel with the pre-prepared filters. The cellulose-rich residue was dried overnight at 60 °C and stored in a desiccator for cellulose recovery determination (Equation 6).

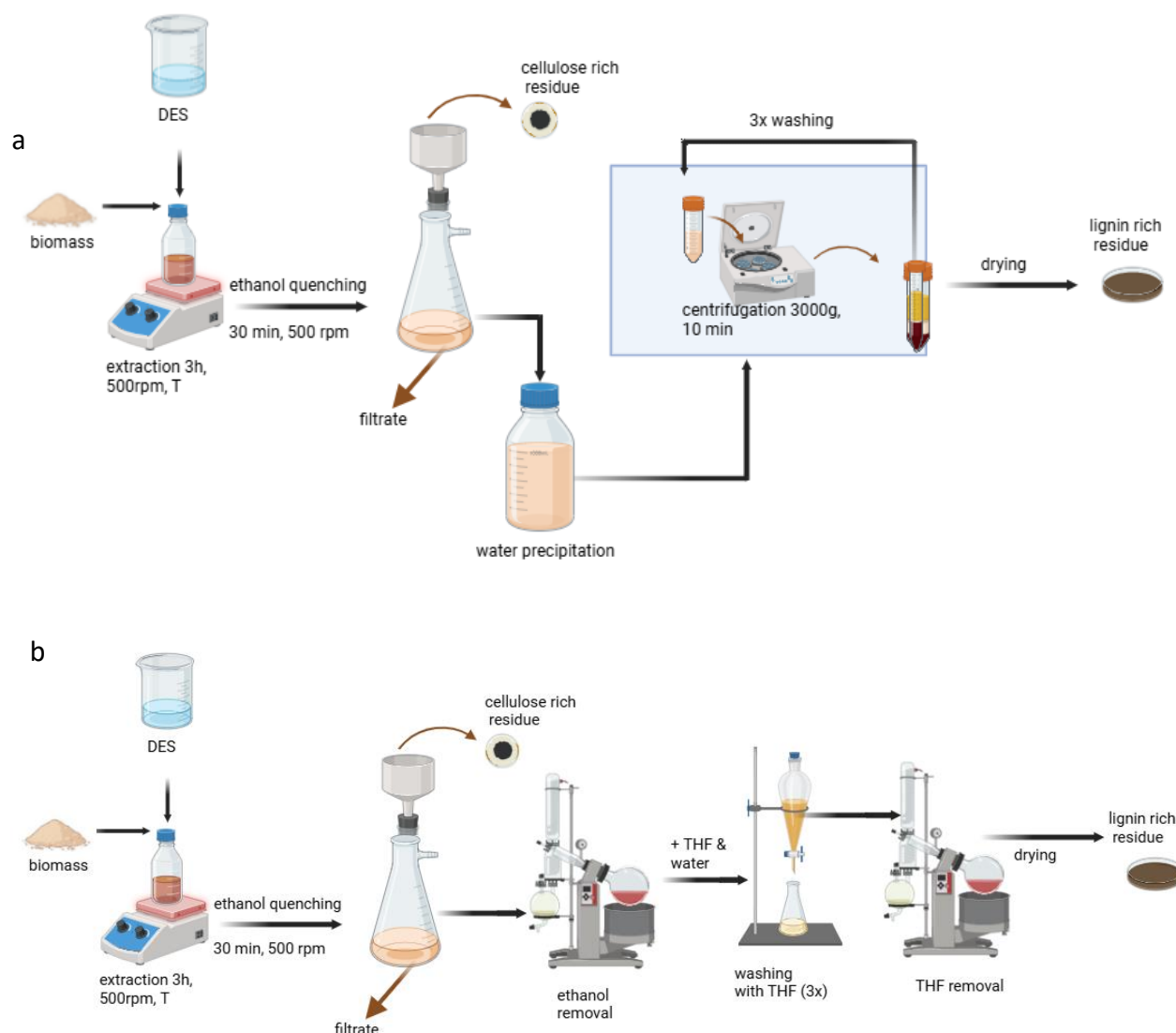


Figure 12: Schematic of lignin extraction from brewery spent grain with (a) ChCl/LA DES and (b) ChCl/EG/OA DES

The filtrate, which contains lignin, DES, and hemicellulose, was collected and ninefold volume of distilled water was added to precipitate lignin at 4 °C overnight. The lignin was recovered by centrifugation at 3000g for 10 minutes. The supernatant was collected and sent to another part of the team for DES recovery. The lignin was further washed to improve its purity. The

washing was done with the previously prepared washing solution (240 ml washing solution for 2 g of biomass) by stirring at 700 rpm for 1 hour. The mixture was centrifuged at 3000g for 10 minutes, and the supernatant was discarded. This washing and centrifugation step was repeated twice to ensure efficient removal of residual DES and hemicellulose.

The final lignin was combined in 20 mL of distilled water in a pre-weighed tube and dried in an oven at 60°C. The final lignin mass was recorded to determine the solid recovery of the lignin rich fraction (Equation 5).

For the ternary DES system (ChCl/EG/OA), lignin was recovered following a solvent extraction procedure adapted from (Liu et al., 2021) as depicted in Figure 12b. According to the authors, the presence of water soluble EG in the ternary DES resulted in a low yield when the precipitation was performed similar to that of ChCl/LA systems. Therefore, after filtering the extract to separate the lignin rich fraction from cellulose rich residue in the same was as for the ChCl/LA DES, the ethanol was removed using a rotary evaporator. To extract lignin, 100 mL of tetrahydrofuran (THF) and 50 mL of distilled water were added, and the mixture was transferred into a separatory funnel. The THF phase (brown-colored, containing lignin) was separated and collected. This extraction was repeated two times with fresh THF. The collected THF phases were combined and concentrated in a rotary evaporator at 40 °C under vacuum. Saturated sodium chloride (brine) was used to precipitate the lignin further by mixing the concentrated THF phase and brine in a separatory funnel. After phase separation, the aqueous (brine) layer was discarded and the THF layer retained. This washing step was repeated two times to improve purity. The final lignin containing phase was dried and weighed.

$$\text{Solid recovery} = \frac{\text{Weight}_{\text{lignin rich solid}}}{\text{Weight}_{\text{biomass}}} \quad (5)$$

$$\text{Cellulose rich residue recovery} = \frac{\text{Weight}_{\text{cellulose rich solid}}}{\text{Weight}_{\text{biomass}}} \quad (6)$$

Table 5: The studied Extraction conditions

Code	DES (molar ratio)	Molar ratio	Extraction T (OC)	Extraction time (h)	Lignin code	Cellulose rich residue code
AG3	ChCl/LA	1:10	100	3	AG3-L	AG3-C
AG4	ChCl/LA	1:10	140	3	AG4-L	AG4-C
AG5	ChCl/LA	1:1	100	3	AG5-L	AG5-C
AG6	ChCl/LA	1:1	140	3	AG6-L	AG6-C
AG7	ChCl/EG/OA	1:2:10w%	100	24	AG7-L	AG7-C

3.2.4. Determination of DES Kamlet-Taft parameters

Kamlet–Taft parameters were determined using three solvatochromic dyes: Nile Red (NR; MW = 318.37 g/mol), 4-nitroaniline (NH₂; MW = 138.13 g/mol), and N,N-diethyl-4-nitroaniline

(NEt₂; MW = 194.23 g/mol). 1 mM stock solution was first prepared by dissolving each dye in methanol. 50 µL of the dye solution was transferred into a centrifugal tube, and the methanol was evaporated using a rotary evaporator under vacuum at 40 °C for 30 minutes. After ethanol removal, 2 mL of the deep eutectic solvent (DES) was added to the tube to dissolve the residual dye and the mixture was homogenized by stirring at 60 °C for 1 hour. Prior to absorbance measurements, the accuracy of UV-Vis spectrophotometer was validated. UV absorbance measurements were recorded between 200 - 800 nm at 25 ± 0.1 °C. The maximum absorption wavelength (λ_{max}) of each dye in the DES was identified and used to calculate the Kamlet–Taft parameters according to empirical equations (7-10) reported by (Zhang et al., 2023b) from which the protocol was adopted.

$$v_{dye} = \frac{10^4}{\lambda_{max,dye}} \quad 7$$

$$polarizability (\pi^*) = 0.314(27.52 - v_{NEt2}) \quad 8$$

$$acidity (\alpha) = \frac{19.9657 - 1.0241\pi^* - v_{NR}}{1.6078} \quad 9$$

$$basicity (\beta) = \frac{1.035v_{NEt2} - 2.64 - v_{NH2}}{2.8} \quad 10$$

3.2.5. FTIR spectroscopy

FTIR spectra were obtained following a direct sampling approach in which a small amount of the sample was directly analyzed using attenuated total reflectance (ATR) with a diamond crystal on a Nicolet 6700 instrument. The parameters of acquisition were: 4 cm⁻¹ resolution, 16 scans per sample, 4000 to 650 cm⁻¹ spectral range. The sample spectrum was collected using Omnic 5.2 software and the data was analyzed in Excel.

3.2.6. NMR spectroscopy

A Bruker AVANCE III 500 MHz NMR equipped was used to acquire 2D HSQC spectra. Around 70 mg of lignin samples were mixed with 0.6 mL deuterated dimethyl sulfoxide (DMSO-d₆). The following parameters were set: 128 transients, 16 dummy scans, a relaxation time of 2.5 s, 1024 data points in the F2 dimension (¹H) and 256 data points in the F1 dimension (¹³C). A ¹JC-H coupling constant of 145 Hz was used. The 2D data set was processed with MestRenova. Data matrices were filled from zero to 1024 points in both dimensions, baseline and phase corrections were applied in both dimensions. The central solvent (DMSO-d₆) was used as the internal chemical shift reference point ($\delta_C/\delta_H = 40.1/2.51$). The following equations (Eq. 11-15) were used to quantify the percentage of sub-units and the main bonds composing the lignin structure from brewery spent grain.

$$Total\ Aromatics = (((S_{2/6} + S'_{2/6})/2) + S_{condensed}) + ((G_2 + G_5 + G_6 - H_{2/6})/3) + (H_{2/6} / 2) \quad (11)$$

$$Ratio\ G = (((G_2 + G_5 + G_6 - H_{2/6})/3) / Total\ Aromatics) \times 100 \quad (12)$$

$$Ratio\ S = (((S_{2/6} + S'_{2/6})/2) + S_{condensed}) / Total\ Aromatics \times 100 \quad (13)$$

$$Ratio\ H = ((H_{2/6}/2) / Total\ Aromatics) \times 100 \quad (14)$$

$$Ix = (Ix / (I_{\beta-O-4} + I_{\beta-\beta} + I_{\beta-5})) \times 100 \quad (15)$$

Where $I_{\beta-O-4}$, $I_{\beta-\beta}$ and $I_{\beta-5}$ correspond to the signals of β -O-4, β - β and β -5 bonds respectively and I_x corresponds to the studied signal.

3.2.7. Klason lignin

Lignin content was determined following the Klason method. The moisture content, ash content, acid insoluble residue (AIR), and acid soluble lignin (ASL) of the extract were determined.

To determine moisture content, approximately 60 mg of dried lignin was weighed into pre-dried and pre-weighed glass tubes and crucibles. They were dried at 105 °C for 24 h, cooled for 1 h in a desiccator, and weighed again. The moisture content was calculated using equation (16)

$$\%moisture = \frac{Weight_{crucible\ plus\ biomass} - Weight_{crucible\ plus\ dry\ biomass}}{Weight_{crucible\ plus\ biomass} - Weight_{crucible}} \times 100 \quad (16)$$

Ash content was measured using the same crucibles by heating them in a muffle furnace at 550 °C (2 h ramp, followed by 2 h at 550 °C, 2h cooling down). After that, the crucibles were cooled in a desiccator for 1 h, and their final weight recorded to determine the ash content as in equation (17).

$$\%ash = \frac{Weight_{crucible\ plus\ ash} - Weight_{crucible}}{ODW_{sample}} \quad (17)$$

For the determination of the AIR and ASL, the samples in glass tubes which were previously used for moisture content determination were used. Glass fiber filters (1.2 μ m) were prepared by placing them in aluminum plates and drying them at 105 °C for 5 h, cooling in a desiccator for 1 h, and weighing. For AIR determination, 0.6 mL of 72% sulfuric acid was added to the samples in glass tubes, heated at 30 °C for 1 h with manual stirring every 10 minutes. Subsequently, 17 mL of distilled water was added to each tube, and the mixtures were autoclaved at 121 °C for 1 h. The hydrolysates were filtered using Büchner funnels fitted with the pre-weighed glass fiber filters. The filtrate was collected. The residue was further washed three times with 10 mL of distilled water, dried at 60 °C for 24 h, cooled in a desiccator for 1 h, and weighed to determine the AIR content.

$$\%AIR = \frac{Weight_{filter\ plus\ residue} - Weight_{filter}}{ODW_{sample}} * 100 \quad (18)$$

$$\%AIL = \%AIR - \%protein_{sample} \quad (19)$$

Where $\%protein_{sample}$ was determined following 3.2.8.

The filtrates were analyzed using UV spectroscopy at 205, 240, and 320 nm to quantify acid-soluble lignin (ASL). Samples with absorbance values exceeding 1 were diluted until an absorbance value less than 1 was obtained. Total lignin content was calculated as the sum of the AIR and ASL fractions.

$$\%ASL = \frac{Volume_{filtrate} * Abs_{320nm} * Dilution\ factor}{ODW_{sample} * \epsilon * path\ length} * 100 \quad (20)$$

Where ϵ is the molar absorptivity in L/(g.cm) and path length refers to the path length of the cuvette in cm.

The total lignin content of the sample is then calculated as the sum of AIL and ASL which is interpreted as the purity of lignin in the stating sample.

3.2.8. Protein content

Protein content was determined using a Flash 2000 elemental analyzer. It was based on CHN analysis to quantify Nitrogen. Sulphanilamide with a known concentration of C, H, and N was used to develop a standard and as control. Approximately 1–2 mg of fine dry samples was weighed into tin capsules and analyzed. Nitrogen percentages obtained from the analysis were converted to protein content using a factor of 6.25, based on the assumption that proteins contain an average of 16% nitrogen. In this analysis, the protein content of raw BSG, hydrothermally pretreated BSG, and AG4-L were determined, and the results are given in Table 6. The protein content of AG4-L was then used as a representative to all other lignin samples.

Table 6: Protein content of different samples as determined by the CHN elemental analysis

Sample	% N	% protein
BSG (raw)	3.0 ± 0.1	18.7 ± 0.7
BSG (Soxhlet plus hydrothermal pretreated)	2.3 ± 1.0	14.28 ± 6.1
AG4-L	1.46 ± 0.1	9.1 ± 0.8

3.2.9. Electrochemical depolymerization

The depolymerization of the lignin samples was performed in an electrochemical setup equipped with a nickel working electrode, a glassy carbon (GC) counter electrode, a Ag/AgCl reference electrode, and a temperature sensor. 1 g/L of a lignin solution was prepared in 0.1 M

NaOH and UV absorbance measured. This medium is known to dissolve lignin and serves as a good electrolyte. 10 mL of this solution was placed in the electrochemical cell under Argon vacuum (to prevent undesired oxidation by atmospheric oxygen). A voltage of 1 V was supplied and the depolymerization was allowed to happen for 4 hours at room temperature. After 4 hours, the solution was collected, and a UV absorbance was measured.

3.2.10. Size exclusion chromatography

Samples were analyzed by size exclusion chromatography (SEC) to assess change in molecular weight distribution after electrochemical depolymerization. For this, samples before and after depolymerization were characterized. 10 μ L of each sample was injected. The mobile phase consisted of aqueous ammonia (pH 10.93), and separation was achieved using two columns with molecular weight ranges of 100–30,000 Da and 100–1,000,000 Da, respectively. The system was equipped with a UV detector set at 280 nm to monitor aromatic lignin species. The analysis was recorded over 40 minutes.

4 Results

4.1. Visual characteristics and Kamlet–Taft parameters of DESs

Three deep eutectic solvents (DESs) with distinct compositions were prepared by heating their respective components between 60–70 °C under magnetic stirring until clear, homogeneous liquids were obtained. Since there was no inert atmosphere to store the DESs, they were immediately consumed. Otherwise, they might absorb water or undergo oxidation which can alter their composition and properties. Visually, the prepared DESs showed clear differences in viscosity. The ternary ChCl/EG/OA DES appeared the most viscous and partially solidified overnight (to avoid this it was used right away). ChCl/LA (1:1) was moderately viscous, while ChCl/LA (1:10) was less viscous as noticed during handling of the DESs. The visually observed trend in viscosity was: ChCl/EG/OA > ChCl/LA (1:1) > ChCl/LA (1:10). Viscosity is generally the drawback faced with many DESs and these preparations showed that it is possible to adjust this parameter by carefully adjusting the components.

In this work, Kamlet-Taft parameters of the three DESs were studied in depth to get a better understanding of their ability to dissolve lignocellulosic biomass. The observed color change of the dyes in different DESs can be seen in Figure 13. This change in color results from differences in the DES's hydrogen bonding interactions with the dye which affects the electronic transitions of the dye molecules. Notably, Nile Red showed visible color changes depending on the DES environment (see Figure 13a).

Moreover, the dipolarity/polarizability (π^*), hydrogen bond donor acidity (α), and hydrogen bond acceptor basicity (β) were quantified, and the results are depicted in Figure 14. Regarding α values, ChCl/LA (1:10) showed the highest α value (1.3). This is expected as lactic acid serves as the primary hydrogen bond donor in the mixture. A high α indicates a highly acidic and strongly protic environment (del Mar Contreras-Gómez et al., 2023). ChCl/LA (1:1) had a slightly lower α value (1.0), while ChCl/EG/OA displayed the lowest α (0.5). The low α value of ChCl/EG/OA implies the hydrogen bond donating ability of this DES is low. In terms of dissolving lignocellulosic biomass, a high α suggests that the solvent can easily disrupt hydrogen-bonding networks in biomass. In contrast, β followed a different trend. ChCl/LA (1:1) exhibited the highest β value (0.7) then followed by ChCl/LA (1:10) with β value of 0.6. while ChCl/EG/OA displayed the lowest β value of 0.4. The difference between α and β is interesting as this number tells us which lignocellulosic component can be dissolved in a particular DES (Alsoy Altinkaya, 2024). ChCl/LA (1:10) exhibited the largest $\alpha - \beta$ value of 0.7 while ChCl/EG/OA showed the smallest value of 0.1, suggesting a more balanced hydrogen bonding environment. Concerning π^* , ChCl/EG/OA recorded the highest π^* value of 1.2. The two ChCl/LA DESs showed similar π^* values close to 1.1. The higher π^* of the ternary DES may arise from the combined effects of ethylene glycol and oxalic acid, which contribute to more complex hydrogen bonding and electron delocalization. In any case, it is fair to say that all three DESs possessed polar environments capable of stabilizing charges.

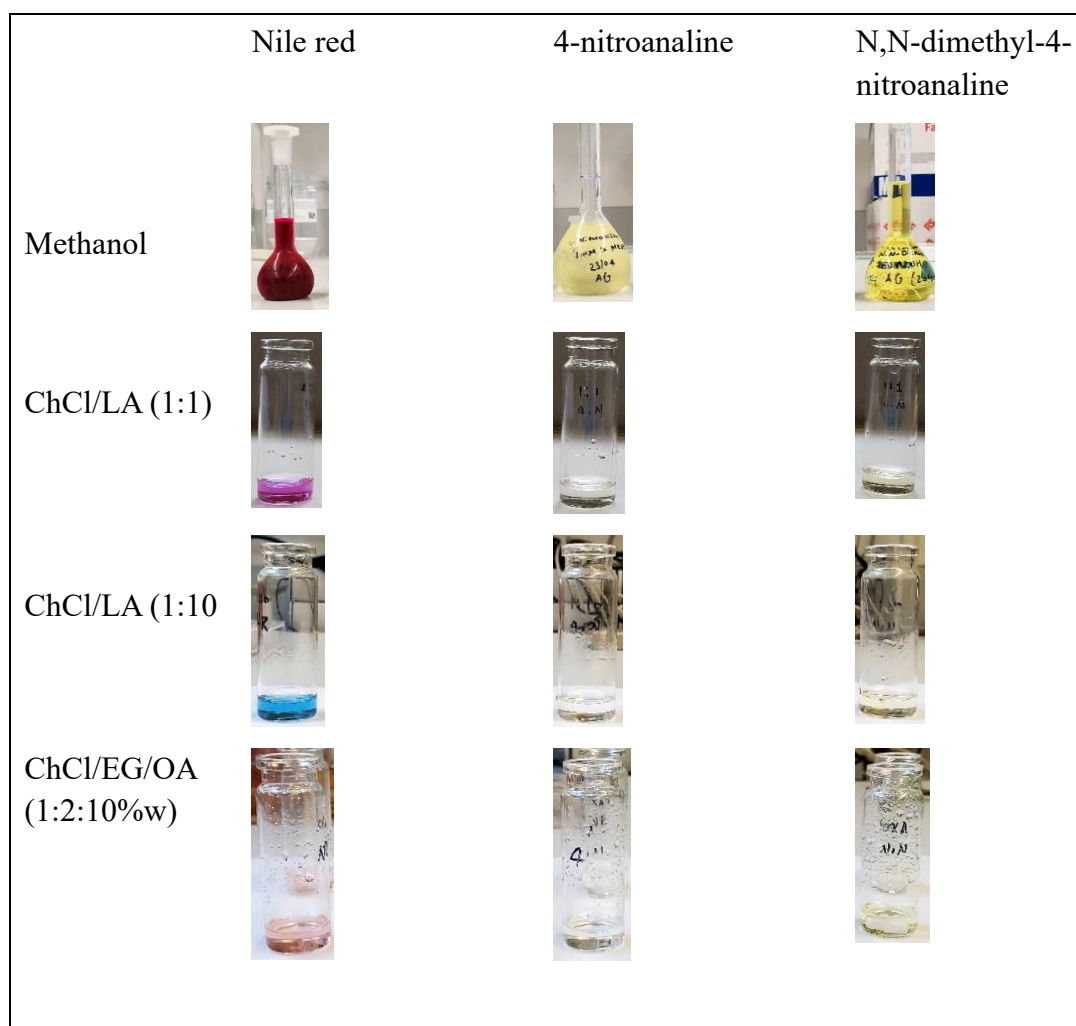


Figure 13: Color change of solvatochromic dyes in the studied DESs and methanol

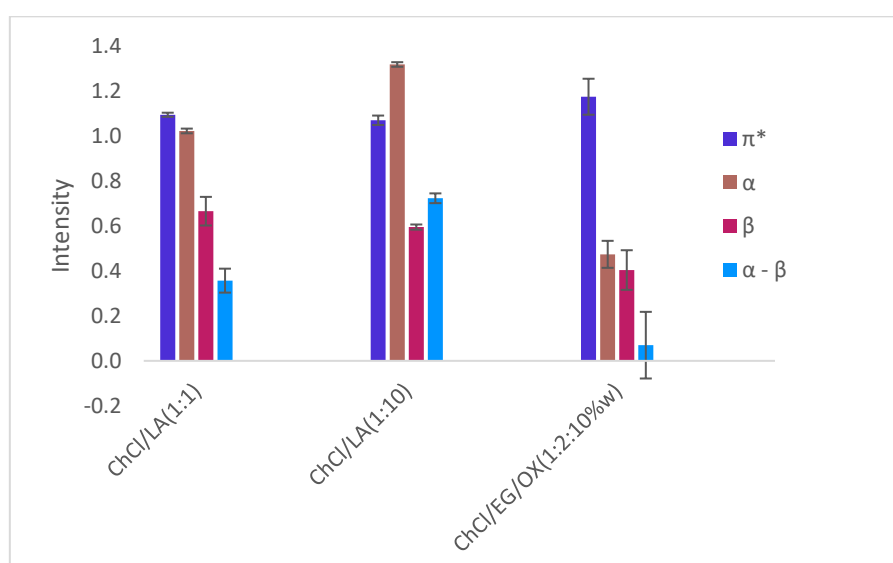


Figure 14: Kamlet-Taft parameters of the studied DESs. The term in paranthesis is the molar ratio of the components

4.2. Extraction results

Lignin extraction from brewery spent grain was carried out using ChCl/LA (AG3 – AG6). For this DES system, two molar ratios (1:1 and 1:10) were investigated at two temperatures (100 or 140°C) for a fixed extraction time (3 h). A ternary DES, ChCl/EG/OA, was also studied for lignin extraction (AG7). The extraction conditions for AG7 were 100°C, 24 h, 500 rpm. Table 4 shows the labels of the samples with their respective extraction conditions.

One observation noticed was that the filtration to recover the lignin rich residue was fast when ChCl/LA with a molar ratio of 1:10 was used for lignin extraction at 100°C. It was slow when a molar ratio of 1:1 was used regardless of the temperature possibly due to the high viscous nature of ChCl/LA DES at this molar ratio. The filtration was even slower for the ternary DES (ChCl/EG/OA) based extraction as this DES system was visually the most viscous. The extraction at 140 °C was characterized by formation of a black lignin fraction. This is commonly observed at high temperatures due to partial degradation and condensation of lignin fragments.

4.2.1. Lignin rich fraction

Figure 15a presents the solid recovery (lignin rich fraction) from different DES systems as calculated from Equation 5. For extraction with ChCl/LA at 1:10 molar ratio, the solid recoveries at 100°C (AG3-L) and 140°C (AG4-L) were 3.3 ± 0.4 and 16.3 ± 4.7 % respectively). For ChCl/LA at 1:1 molar ratio (AG5-L and AG6-L), the values were 1.7 ± 0.2 and 22.3 ± 0.9 % respectively. It can be noticed that increasing the molar ratio of ChCl/LA and the extraction temperature increased the solid recovery for this DES system. The increase is more pronounced with temperature. For the ternary DES system ChCl/EG/OA (AG7-L), the highest solid recovery rate of 70.4 ± 8.9 % was recorded. However, it is important to note that this value cannot be directly compared to the ChCl/LA system as the extraction time was longer (24 h versus 3 h).

Figure 15b shows the lignin purity of the recovered solid fractions. For the ChCl/LA DES system, the purity values (%) were 79.0 ± 0.2 for AG3-L, 79.2 ± 2.5 for AG4-L, and 83.6 ± 2.6 for AG6-L. The values show that the purity wasn't affected much by temperature where as changing the molar ratio from 1:10 to 1:1 slightly enhanced it (AG4-L versus AG6-L). Purity data for AG5-L are not available as the mass extracted wasn't enough to perform the Klason protocol (six duplicate extractions were required to recover enough solid which was not possible due to time constraints). In contrast, the ternary DES system ChCl/EG/OA (AG7-L) resulted in a significantly lower lignin purity of 11.3 ± 4.0 . Although AG7-L provided the highest solid recovery (as shown in Figure 13a), the recovered material contained a large proportion of non-lignin components. This was also visually confirmed as the recovered material was gel like as opposed to the one extracted with ChCl/LA (powder like).

Lignin yield is another parameter investigated for recovered solid. This considers the true lignin content both in the recovered solid and in the initial biomass and is equal to Klason lignin (see Methods).

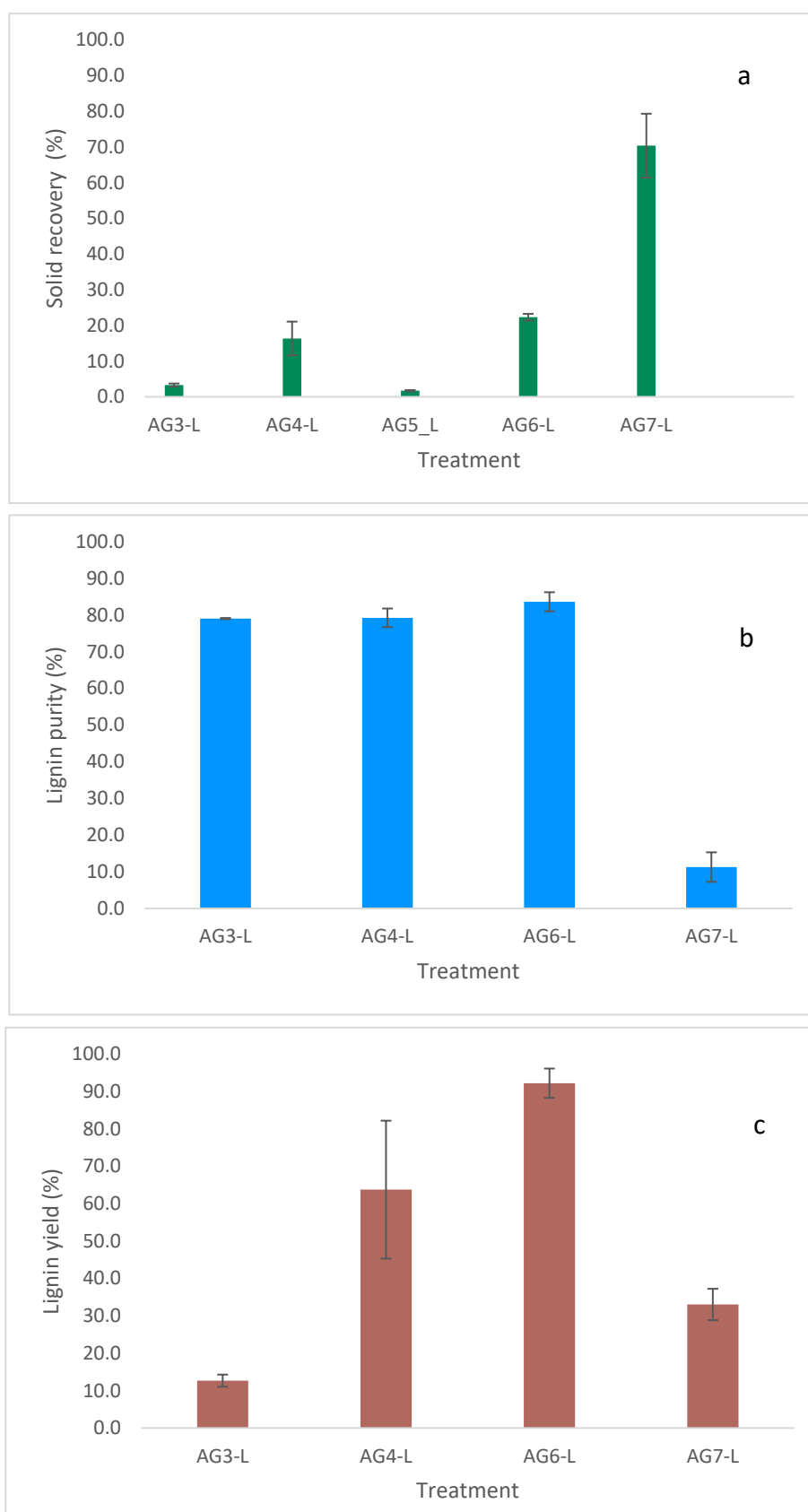


Figure 15: Lignin extraction from brewery spent grain with different DES at 100 and 140 °C: a) solid recovery b) purity c) lignin yield ; Note that purity and yield of AG5-L was not determined

Figure 15c shows the actual lignin yield of the different extracts. For ChCl/LA at a 1:10 molar ratio, the yield increased from 12.7 ± 1.6 % at 100 °C (AG3-L) to 63.7 ± 18.4 % at 140 °C (AG4-L). The lignin yield was 92.2 ± 3.9 % for the 1:1 molar ratio at 140 °C (AG6-L) whereas no lignin yield data was obtained at 100 °C (for reasons mentioned before). These results show that both high temperature and low ChCl/LA molar ratio improve the lignin yield. The ternary DES system ChCl/EG/OA (AG7-L) gave a yield of 33.0 ± 4.2 %, which was higher than AG3-L but lower than AG4-L and AG6-L.

4.2.2. Cellulose rich fraction

The cellulose rich fraction was the solid that was retained in the filter when filtering the extract. The yield of this residue is calculated based on Equation 6 and the values are given in Figure 16. The values were 161.0 ± 3.2 %, 108.8 ± 3.5 , 73.8 ± 14.3 %, 162.4 ± 12.3 %, 131.9 ± 37.9 % for AG3-C, AG4-C, AG5-C, AG6-C, and AG7-C respectively. The occurrence of values exceeding 100% is due to the possible retention of residual DES components or other non-cellulosic material in the cellulose rich fraction. This indicates this fraction is not purely cellulose, and further analysis of this fraction is recommended to quantify cellulose content. Purification and characterization of the cellulose rich residue was beyond the scope of this work.

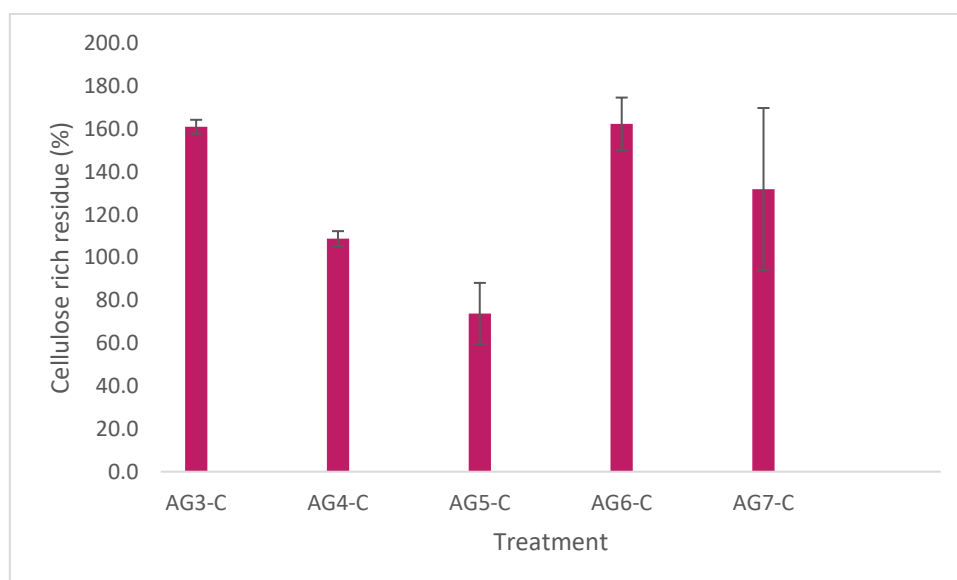


Figure 16: Cellulose rich residue obtained after lignin extraction with different DESs at 100 or 140°C

4.2.3. FTIR spectra

Figure 17 shows the FTIR spectra of the lignin samples discussed before. All samples showed characteristic lignin absorption bands. A broad peak around 3306 cm^{-1} was assigned to O–H stretching vibrations of phenolic and aliphatic hydroxyl groups. The bands at 2921 and 2846 cm^{-1} respectively correspond to C–H stretching in methyl ($-\text{CH}_3$) and methylene ($-\text{CH}_2-$) groups. The bands specific to lignin can be seen by zooming out in the region 1800 to 800 cm^{-1} , also known as the fingerprint region (see right side of Figure 17). Typical lignin aromatic

skeletal vibrations can be seen around 1630 and 1510 cm^{-1} , while the band at 1450 cm^{-1} is associated with CH_2 deformations. The presence of syringyl (S) and guaiacyl (G) units is supported by peaks at 1265 cm^{-1} , 1126 cm^{-1} , and 1029 cm^{-1} , which are associated with C–O stretching in aromatic methoxyl and ether linkages. Some slight differences in the FTIR spectra of the lignin samples extracted with ChCl/LA DES (AG3-L to AG6-L) can give us some insights into the effect of the extraction conditions. For example, increasing the temperature from 100 °C to 140 °C at the same molar ratio (AG3-L to AG4-L or AG5-L to AG6-L) led to slightly more defined peaks in the aromatic skeletal region. This can be the result of improved purity at higher extraction times. Lignin extracted with the ternary DES (AG7-L) showed broader and more intense signals which may suggest the presence of DES residues, consistent with its lower purity. The broader peak around 3306, for example, may be intensified by the OH groups coming from ethylene glycol.

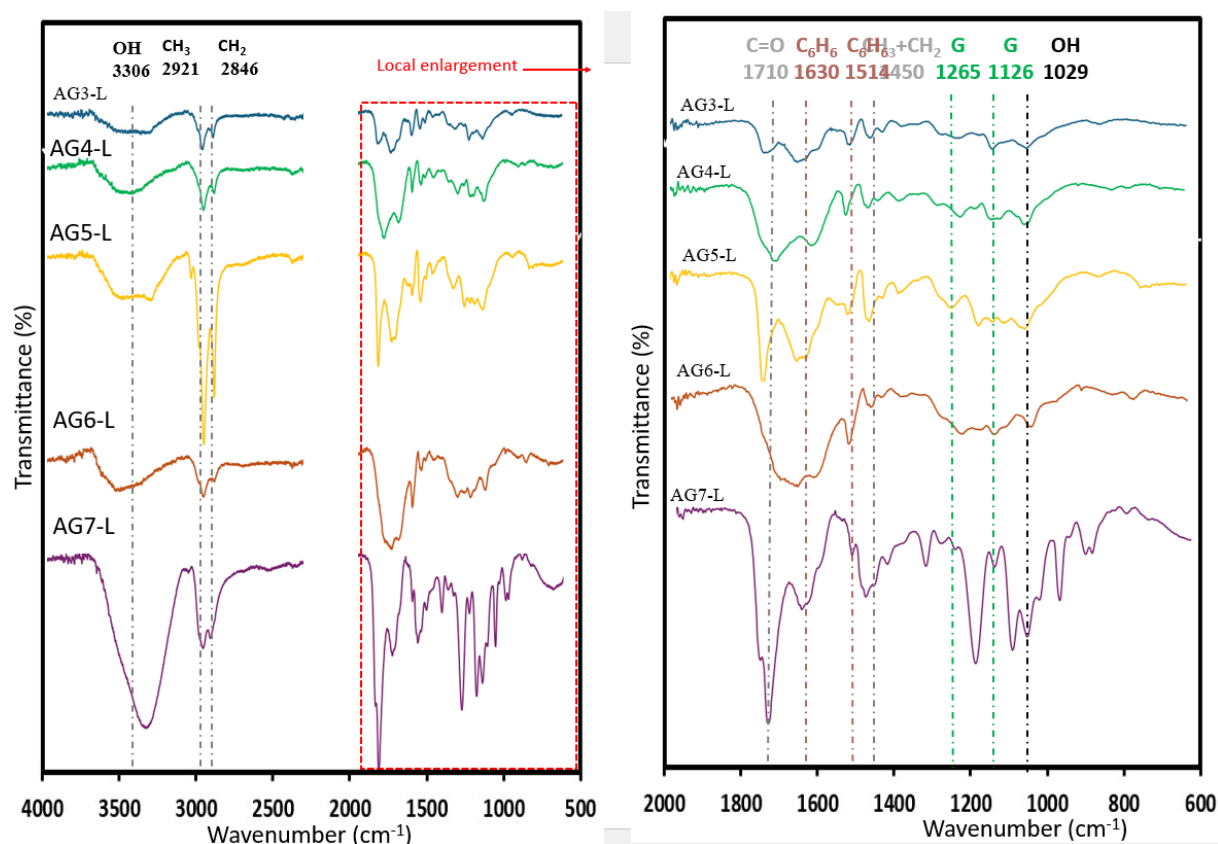


Figure 17: FTIR spectra of different lignin extracted with different DES at 100 °C or 140 °C

4.2.4. NMR spectra

The 2D HSQC NMR spectra of lignin extracted from BSG at 140 °C with ChCl/LA (1:10) and ChCl/LA (1:1) is presented in Figure 18. The NMR spectra of the other samples weren't available until the submission date of this report. Both spectra reveal the presence of major interunit linkages typical of lignin, including β -O-4 (aryl ether), β - β (resinol), and β -5 (phenylcoumaran) structures. Two regions can be identified in the spectra: the aromatic region and the aliphatic region. In the aromatic region, AG4-L displays signals corresponding to

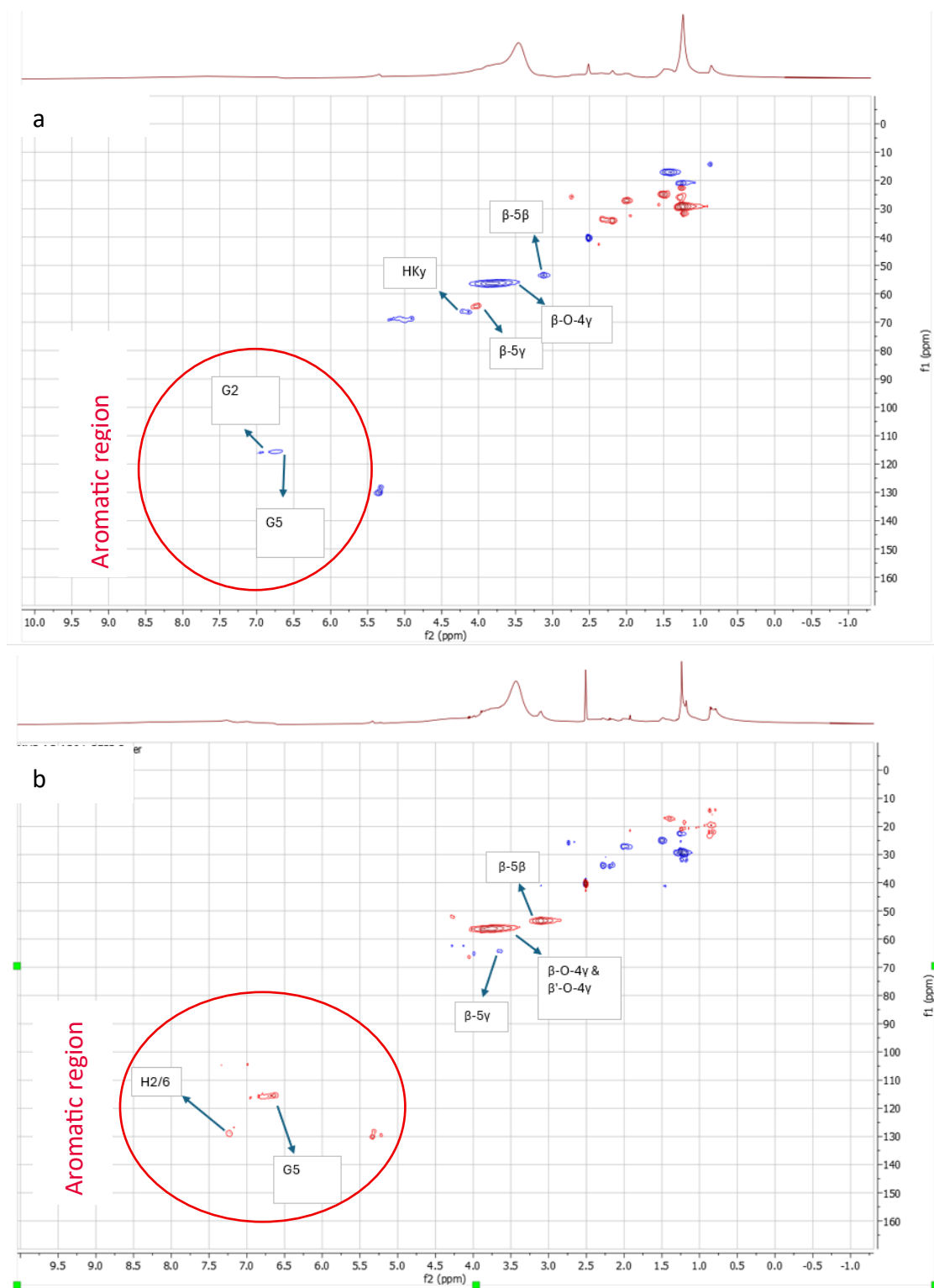


Figure 18: NMR spectra of lignin extracted at 140 °C with ChCl/LA having molar ratio of (a) 1:10 (AG4-L) and b) 1:1 (AG6-L)

guaiacyl units (G) and some hydroxyphenyl (H) units. AG6-L also shows G and H signals. The aliphatic region shows the presence of β -O-4 and β -5 linkages in both samples. AG4-L also shows β - β signals. This may reflect differences in depolymerization and solubilization behavior influenced by the molar ratio of the DES. In both spectra, No syringyl (S) signals were detected in both samples. This is likely because this subunit is degraded at high temperatures (140°C) as also reported in the literature (Hong et al., 2020a).

The quantification of the different linages in the lignin samples is important to know the influence of the extraction conditions on lignin structure. This is the next task of this work, and the different bonds will be quantified according to equations (9-13). Once the quantities are determined, it is possible to say which of the conditions are preserving the linkages in lignin, in particular the β -O-4 linkages, which is interesting in lignin depolymerization.

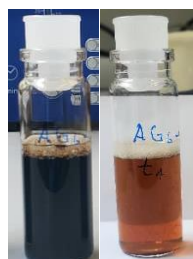
4.3. Electrochemical depolarization

The goal of this experiment was to explore the potential for electrochemical depolymerization of lignin samples, particularly those that preserve β -O-4 linkages. Identifying such lignins requires full NMR characterization, which is still in progress. For the purpose of this report, one lignin sample (AG6-L), extracted with ChCl/LA (1:1) at 140 °C, was selected for preliminary electrochemical depolymerization. The electrochemical depolymerization was done for 4h in 0.1M NaOH solution. Figure 19 depicts the results.

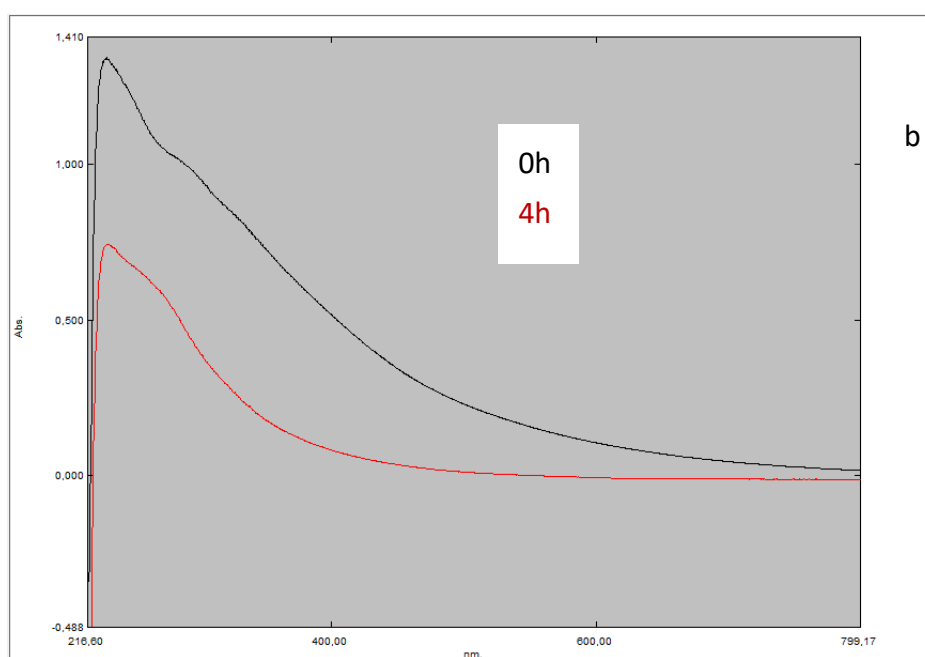
As shown in Figure 19a, a visible color change from dark brown (0 h) to light orange (4 h) was observed. This indicates that a chemical transformation of the lignin solution during depolymerization has happened.

Figure 19b shows the corresponding UV absorbance spectra recorded before and after the reaction. Lignin is known to absorb in the UV-Vis region due to its aromatic and phenolic structures. Lignin's UV spectra show a maximum absorption in around 280 nm. This absorption maximum is due to non-conjugated phenolic groups and aromatic ring $\pi \rightarrow \pi$ transitions (Tian et al., 2015). A peak around 210 nm is also common for lignin attributable to phenolic content. These absorbance peaks are used to monitor the degradation of lignin (be it enzymatic or chemical degradation). For AG6-L, the initial spectrum showed a big absorbance peak around 280 nm in line with expectations. After 4 hours of electrolysis, the absorbance intensity decreased, suggesting degradation of aromatic rings. The color changes supplemented with the reduction in absorbance tell us that a cleavage of interunit linkages has taken place and smaller fragments have possibly formed. This is a good clue to proceed studying further electrochemical depolymerization. Figure 19c shows the SEC chromatogram before and after depolymerization for AG6-L (ChCl/LA (1:1) ,140°C, 3h) detected by UV. The UV signal of the untreated lignin exhibited a single dominant peak corresponding to high-molecular-weight aromatic species. After 4 h of electrochemical depolymerization, the UV trace revealed two distinct peaks: one at the original retention time and another shifted to later times, indicative of lower-molecular-weight fragments.. However, the exact molecular weights were not determined as UV detector isn't convenient for this purpose.

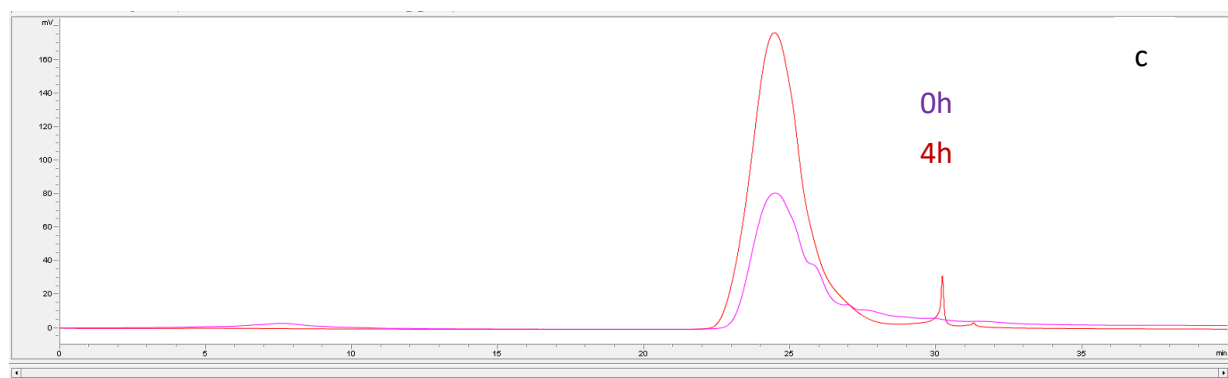
0h 4h



a



b



c

Figure 19: Comparing before and after electrochemical depolymerization AG6-L (ChCl/LA (1:1) , 140°C: 3h):
a) color change, b) UV absorbance, c) SEC elution profile as a function of retention time

5 Discussion of results

5.1. Effect of extraction conditions on lignin yield

The effectiveness of lignin extraction from BSG was affected by both the composition of DES and extraction temperature. For example, changing the molar ratio of ChCl/LA from 1:1 to 1:10 at 100 °C increased the solid recovery rate from 1.7 % to 3.3 %. Other authors have reported similar trends. Zhang et al., (2016) showed that modifying the ChCl/LA molar ratio from 1:2 to 1:10 led to an increase in lignin yield from 63.7% to 93.1%, which they attributed to improved solvent acidity and hydrogen bonding capabilities. This is also in line with the prediction using Kamlet-Taft parameters. The ChCl/LA (1:10) system exhibited higher $\alpha - \beta$ value among the consistent with its superior solid recovery.

Temperature had even a more pronounced effect in lignin yield. Lignin extraction from BSG with ChCl/LA (1:10) yielded 12.7 % at 100 °C and 63.7 % at 140 °C consistent with literature findings. Cassoni et al. (2023), One study on lignin extraction from BSG using ChCl:LA (1:5) DES showed that increasing the temperature from 60 °C to 120 °C improved lignin yield from 18.3% to 58.6% (Cassoni et al., 2023b). The increased lignin yield with increasing temperature is primarily due to enhanced mass transfer at high temperatures which again improves solubilization of lignin in the solvent. High temperature also promotes bond cleavage within the lignin polymer network (Cassoni et al., 2023b; Rodrigues et al., 2024).

The reduced purity (despite high solid recovery) and viscous nature of the lignin extracted using the ternary DES (ChCl/EG/OA) can result from different factors. First, the moderate acidity and high basicity (low α , high β) of this DES favors the solubilization of not only lignin but also hemicelluloses and other components. Second, the lower extraction temperature (100 °C) may have limited lignin solubilization efficiency. Lastly, the prolonged extraction time (24 h) may have led to condensation or polymerization reactions forming a gel-like solid. Liu et al., (2021) reported similar characteristics of lignin extracted with the same ternary DESs and extraction conditions.

5.2. Structural features of lignin

The FTIR spectra of the DES-extracted lignins revealed characteristic lignin functional groups as presented in Figure 17 which are quite comparable to other spectra in the literature (Fernandes et al., 2024; Provost et al., 2022). The spectra of all ChCl/LA extracted show slight differences. The slightly stronger signals around 1510 and 1700 cm^{-1} for lignin extracted at 140 °C (AG4-L and AG6-L) compared to at 100 °C (AG3-L and AG6-L) may result from condensation reactions which is typical for lignin at high temperatures (Kačík et al., 2025). However, changing the molar ratio at the same temperature didn't seem to change the intensity of the observed signals.

The 2D HSQC NMR analysis confirmed the presence of aromatic and aliphatic linkages in lignin samples extracted with ChCl/LA in both molar ratios at 140 °C. The presence of β -O-4 linkages was also detected but their quantities isn't determined yet. The interpretation of the NMR results is limited due to the unavailability of spectra for samples extracted at 100 °C. This missing data limits our ability to assess how milder extraction conditions influence the structural preservation of lignin, particularly the thermally sensitive β -O-4 linkages. The preservation of these bonds is interesting for lignin valorization by depolymerization. Studies

have shown that extraction conditions significantly affect the retention of native lignin structures. Lower-temperature paired with less acidic DES systems tend to favor β -O-4 preservation (Chen et al., 2020c; Li et al., 2024). In this work, that would mean the lignin extracted with ChCl/LA (1:1) at 100 °C but we can only tell after a complete characterization of the samples. In contrast, high temperatures and acidic conditions promote cleavage of labile bonds leading to more recalcitrant lignin structures (Kačík et al., 2025). This shows the tradeoff between high lignin yield and preservation of β -O-4 linkages.

Although the NMR spectra of the ChCl/EG/OA extracted lignin (AG7-L) isn't present, a study by Liu et al., (2021) with the same DES and same extraction conditions revealed the preservation of high β -O-4 linkages by incorporating ethylene glycol into the lignin structure thereby suppressing recondensation. HSQC NMR analysis of their sample revealed up to 53 β -O-4 linkages (both native and modified) per 100 aromatic units. This number was higher than in lignin extracted with traditional acidic DESs. This demonstrates that despite the low purity of the ternary DES extracted lignin, it can be interesting from the point of view of preserving β -O-4 linkages and by extension for electrochemical valorization if confirmed.

5.3. Electrochemical depolymerization of lignin

The preliminary results of electrochemical depolymerization suggest a promising potential for breaking down lignin under greener conditions (mild temperature). In this work, only the lignin extracted with ChCl/LA (1:1, 140 °C, 3h) was tested due to absence of complete NMR data and time constraints. The observed color change accompanied by a notable decrease in UV absorbance at around 280 nm is possibly due to a reduction in aromatic ring systems caused by oxidative or reductive cleavage of interunit linkages such as β -O-4. UV-vis and visual observations provide initial qualitative evidence for depolymerization, but they do not confirm the formation of low molecular weight products. The change in absorbance could also arise from repolymerization or condensation reactions, especially in lignin samples where reactive intermediates (e.g., phenoxy radicals) are not stabilized (Borba et al., 2016). SEC chromatogram also shows the appearance of peaks at a longer retention time. However, the intensity of the big MW fragments increased relative to the 0 h sample in the SEC chromatogram. Since the SEC signals were detected by UV at 280 nm and UV only shows the aromatic rings, the relative increase may not mean anything in terms of molecular weight. Alternatively, this could mean that in addition to fragmentation, condensation reactions have occurred during electrolysis. The true average MW of the fragments was not determined as the equipment was now fitted with a suitable detector. The nature and quantities of the fragments will be studied by GC-MS in the remaining time of the internship.

It is important to note that the success of electrochemical depolymerization depends on the structure, particularly in the β -O-4 linkages of the lignin sample. Other studies have demonstrated the role of lignin structure in lignin electrochemical depolymerization. For example, Alves da Cruz et al., (2022) demonstrated that organosolv lignin with high content of β -O-4 linkages could be selectively depolymerized using anodic oxidation. Their work showed that the process yielded valuable monomers such as guaiacol, vanillin, and syringaldehyde. They also showed that parameters like the applied potential and electrode material influenced product distribution. Similarly, Zhang (2022) emphasized the importance of β -O-4-rich lignins for successful depolymerization, noting that highly condensed technical lignins such as kraft

lignin exhibit poor reactivity under electrochemical conditions. Zhang's findings also underline the influence of lignin extraction methods on structural preservation. They pointed out that mild protocols like organosolv or DES are preferred to preserve labile linkages.

6 Conclusion and feature perspectives

In this study, the extraction and characterization of lignin from brewery spent grain with ChCl/LA (1:1 and 1:10 molar ratios) and ChCl/EG/OA was performed with emphasis on the effect of molar ratio and temperature on solid recovery, purity, and yield. Among the ChCl/LA DES, higher temperature (140 °C) led to increased solid recovery and lignin yields. It wasn't possible to conclude on the effect of molar ratio on solid recovery, yield and purity due to conflicting data at 100 and 140°C. Interestingly, the lignin purity remained similar among all samples extracted with ChCl/LA DES. However, the purity was low for the ternary DES extracted lignin (Ag7-L). The FTIR spectra of AG7-L also showed broader and more intense signals compared to the others possibly due to the presence of impurities such as residual DES. It was also preliminarily shown that one of the lignin samples (ChCl/LA, 1:1, 140°C, 3h) can be electrochemically broken down into smaller monomers as observed by its color change and reduced UV absorbance after electrolysis. This is an interesting starting point to proceed further with identification and quantification of the monomers.

The future work, therefore, will focus on completing the characterization of the lignin samples to better understand their structure. The extracted lignin samples will be depolymerized to establish a structure-depolymerization efficiency relationship. Focus will be given to studying the effect of β -O-4 linkages on electrochemical depolymerization efficiency of samples. All the extraction and characterization experiments will be repeated on grape pomace, a biomass that is known to exhibit different compositions compared to brewery spent grain. This will give a comparative study for process development.

7 References

- Abu-Omar, M.M., Barta, K., Beckham, G.T., Luterbacher, J.S., Ralph, J., Rinaldi, R., Román-Leshkov, Y., Samec, J.S.M., Sels, B.F., Wang, F., 2021. Guidelines for performing lignin-first biorefining. *Energy Environ Sci.* <https://doi.org/10.1039/d0ee02870c>
- Alonso, D.A., Baeza, A., Chinchilla, R., Guillena, G., Pastor, I.M., Ramón, D.J., 2016. Deep Eutectic Solvents: The Organic Reaction Medium of the Century. *European J Org Chem.* <https://doi.org/10.1002/ejoc.201501197>
- Alsoy Altinkaya, S., 2024. A perspective on cellulose dissolution with deep eutectic solvents. *Frontiers in Membrane Science and Technology* 3. <https://doi.org/10.3389/fmst.2024.1382054>
- Alves da Cruz, M.G., Gueret, R., Chen, J., Piątek, J., Sipponen, M., Frauscher, M., Budnyk, S., Rodrigues, B., Slabon, A., 2022. Electrochemical Depolymerization of Lignin in a Biomass-based Solvent. <https://doi.org/10.26434/chemrxiv-2022-9164j>
- Arni, S. Al, 2018. Extraction and isolation methods for lignin separation from sugarcane bagasse: A review. *Ind Crops Prod.* <https://doi.org/10.1016/j.indcrop.2018.02.012>
- Ayub, R., Raheel, A., 2022. High-Value Chemicals from Electrocatalytic Depolymerization of Lignin: Challenges and Opportunities. *Int J Mol Sci.* <https://doi.org/10.3390/ijms23073767>
- Bajpai, P., 2016. Structure of Lignocellulosic Biomass. pp. 7–12. https://doi.org/10.1007/978-981-10-0687-6_2
- Bertella, S., Luterbacher, J.S., 2020. Lignin Functionalization for the Production of Novel Materials. *Trends Chem.* <https://doi.org/10.1016/j.trechm.2020.03.001>
- Borba, A., Almangano, M., Portugal, A.A., Patrício, R., Simões, P.N., 2016. Methylsilsesquioxane-Based Aerogel Systems - Insights into the Role of the Formation of Molecular Clusters. *Journal of Physical Chemistry A* 120, 4079–4088. <https://doi.org/10.1021/acs.jpca.6b04196>
- Bourbiaux, D., Pu, J., Rataboul, F., Djakovitch, L., Geantet, C., Laurenti, D., 2021. Reductive or oxidative catalytic lignin depolymerization: An overview of recent advances. *Catal Today* 373, 24–37. <https://doi.org/10.1016/j.cattod.2021.03.027>
- Cassoni, A.C., Costa, P., Mota, I., Vasconcelos, M.W., Pintado, M., 2023a. Recovery of lignins with antioxidant activity from Brewer's spent grain and olive tree pruning using deep eutectic solvents. *Chemical Engineering Research and Design* 192, 34–43. <https://doi.org/10.1016/j.cherd.2023.01.053>
- Cassoni, A.C., Costa, P., Mota, I., Vasconcelos, M.W., Pintado, M., 2023b. Recovery of lignins with antioxidant activity from Brewer's spent grain and olive tree pruning using deep eutectic solvents. *Chemical Engineering Research and Design* 192, 34–43. <https://doi.org/10.1016/j.cherd.2023.01.053>
- Cassoni, A.C., Costa, P., Vasconcelos, M.W., Pintado, M., 2022. Systematic review on lignin valorization in the agro-food system: From sources to applications. *J Environ Manage.* <https://doi.org/10.1016/j.jenvman.2022.115258>
- Chen, M., Li, Y., Liu, H., Zhang, D., Shi, Q.S., Zhong, X.Q., Guo, Y., Xie, X.B., 2023. High value valorization of lignin as environmental benign antimicrobial. *Mater Today Bio.* <https://doi.org/10.1016/j.mtbio.2022.100520>

- Chen, Z., Bai, X., Lusi, A., Zhang, H., Wan, C., 2020a. Insights into Structural Changes of Lignin toward Tailored Properties during Deep Eutectic Solvent Pretreatment. *ACS Sustain Chem Eng* 8, 9783–9793. <https://doi.org/10.1021/acssuschemeng.0c01361>
- Chen, Z., Ragauskas, A., Wan, C., 2020b. Lignin extraction and upgrading using deep eutectic solvents. *Ind Crops Prod.* <https://doi.org/10.1016/j.indcrop.2020.112241>
- Chen, Z., Ragauskas, A., Wan, C., 2020c. Lignin extraction and upgrading using deep eutectic solvents. *Ind Crops Prod.* <https://doi.org/10.1016/j.indcrop.2020.112241>
- Cheng, J., Chen, T., Liu, X., Zhou, X., Zhan, Y., Huang, C., Cao, X., Fang, G., Huang, C., 2024. A lignin-first biorefinery by integrated deep eutectic solvents towards formaldehyde-free plywood adhesive and monomeric sugars. *Chemical Engineering Journal* 499. <https://doi.org/10.1016/j.cej.2024.155980>
- Chio, C., Sain, M., Qin, W., 2019. Lignin utilization: A review of lignin depolymerization from various aspects. *Renewable and Sustainable Energy Reviews.* <https://doi.org/10.1016/j.rser.2019.03.008>
- del Mar Contreras-Gómez, M., Galán-Martín, Á., Seixas, N., da Costa Lopes, A.M., Silvestre, A., Castro, E., 2023. Deep eutectic solvents for improved biomass pretreatment: Current status and future prospective towards sustainable processes. *Bioresour Technol.* <https://doi.org/10.1016/j.biortech.2022.128396>
- Dwamena, A.K., Raynie, D.E., 2020. Solvatochromic Parameters of Deep Eutectic Solvents: Effect of Different Carboxylic Acids as Hydrogen Bond Donor. *J Chem Eng Data* 65, 640–646. <https://doi.org/10.1021/acs.jced.9b00872>
- Feofilova, E.P., Mysyakina, I.S., 2016. Lignin: Chemical structure, biodegradation, and practical application (a review). *Appl Biochem Microbiol.* <https://doi.org/10.1134/S0003683816060053>
- Fernandes, C., Aliaño-González, M.J., Cid Gomes, L., Bernin, D., Gaspar, R., Fardim, P., Reis, M.S., Alves, L., Medronho, B., Rasteiro, M.G., Varela, C., 2024. Lignin extraction from acacia wood: Crafting deep eutectic solvents with a systematic D-optimal mixture-process experimental design. *Int J Biol Macromol* 280. <https://doi.org/10.1016/j.ijbiomac.2024.135936>
- Garedew, M., Lam, C.H., Petitjean, L., Huang, S., Song, B., Lin, F., Jackson, J.E., Saffron, C.M., Anastas, P.T., 2021. Electrochemical upgrading of depolymerized lignin: a review of model compound studies. *Green Chemistry* 23, 2868–2899. <https://doi.org/10.1039/d0gc04127k>
- Hansen, B.B., Spittle, S., Chen, B., Poe, D., Zhang, Y., Klein, J.M., Horton, A., Adhikari, L., Zelovich, T., Doherty, B.W., Gurkan, B., Maginn, E.J., Ragauskas, A., Dadmun, M., Zawodzinski, T.A., Baker, G.A., Tuckerman, M.E., Savinell, R.F., Sangoro, J.R., 2021. Deep Eutectic Solvents: A Review of Fundamentals and Applications. *Chem Rev.* <https://doi.org/10.1021/acs.chemrev.0c00385>
- He, C., Luo, F., Zhu, Y., Zhan, A., Fan, J., Clark, J.H., Lv, J., Yu, Q., 2025. A “lignin-first” biorefinery towards efficient aromatic monomer conversion from coconut shells using mild TMAH-based alkaline deep eutectic solvents. *Green Chemistry.* <https://doi.org/10.1039/d4gc05498a>

- Hong, S., Shen, X.J., Sun, Z., Yuan, T.Q., 2020a. Insights into Structural Transformations of Lignin Toward High Reactivity During Choline Chloride/Formic Acid Deep Eutectic Solvents Pretreatment. *Front Energy Res* 8. <https://doi.org/10.3389/fenrg.2020.573198>
- Hong, S., Shen, X.J., Xue, Z., Sun, Z., Yuan, T.Q., 2020b. Structure-function relationships of deep eutectic solvents for lignin extraction and chemical transformation. *Green Chemistry*. <https://doi.org/10.1039/d0gc02439b>
- Jose, D., Tawai, A., Divakaran, D., Bhattacharyya, D., Venkatachalam, P., Tantayotai, P., Sriariyanun, M., 2023. Integration of deep eutectic solvent in biorefining process of lignocellulosic biomass valorization. *Bioresour Technol Rep*. <https://doi.org/10.1016/j.biteb.2023.101365>
- Kačík, F., Výbohová, E., Jurczyková, T., Eštoková, A., Kmet'ová, E., Kačíková, D., 2025. Impact of Thermal Treatment and Aging on Lignin Properties in Spruce Wood: Pathways to Value-Added Applications. *Polymers* (Basel) 17. <https://doi.org/10.3390/polym17020238>
- Khalili, K.N.M., de Peinder, P., Donkers, J., Gosselink, R.J.A., Bruijninx, P.C.A., Weckhuysen, B.M., 2021. Monitoring Molecular Weight Changes during Technical Lignin Depolymerization by Operando Attenuated Total Reflectance Infrared Spectroscopy and Chemometrics. *ChemSusChem* 14, 5517–5524. <https://doi.org/10.1002/cssc.202101853>
- Kropat, M., Liao, M., Park, H., Salem, K.S., Johnson, S., Argyropoulos, D.S., 2021. Lignin processing & utilization, *BioResources*.
- Li, P., Zhang, Z., Zhang, X., Li, K., Jin, Y., Wu, W., 2023. DES: their effect on lignin and recycling performance. *RSC Adv*. <https://doi.org/10.1039/d2ra06033g>
- Li, W., Ma, S., Luo, L., Li, Z., He, A., Wang, C., Lin, L., Zeng, X., 2024. Pretreatment of biomass with ethanol/deep eutectic solvent towards higher component recovery and obtaining lignin with high β -O-4 content. *Int J Biol Macromol* 276. <https://doi.org/10.1016/j.ijbiomac.2024.133751>
- Liang, X., Zhu, Y., Qi, B., Li, S., Luo, J., Wan, Y., 2021. Structure-property-performance relationships of lactic acid-based deep eutectic solvents with different hydrogen bond acceptors for corn stover pretreatment. *Bioresour Technol* 336. <https://doi.org/10.1016/j.biortech.2021.125312>
- Liao, J.J., Latif, N.H.A., Trache, D., Brosse, N., Hussin, M.H., 2020. Current advancement on the isolation, characterization and application of lignin. *Int J Biol Macromol*. <https://doi.org/10.1016/j.ijbiomac.2020.06.168>
- Liu, Q., Zhao, X., Yu, D., Yu, H., Zhang, Y., Xue, Z., Mu, T., 2019. Novel deep eutectic solvents with different functional groups towards highly efficient dissolution of lignin. *Green Chemistry* 21, 5291–5297. <https://doi.org/10.1039/c9gc02306b>
- Liu, W., Chen, W., Hou, Q., Wang, S., Liu, F., 2018. Effects of combined pretreatment of dilute acid pre-extraction and chemical-assisted mechanical refining on enzymatic hydrolysis of lignocellulosic biomass. *RSC Adv* 8, 10207–10214. <https://doi.org/10.1039/c7ra12732d>
- Liu, Y., Deak, N., Wang, Z., Yu, H., Hameleers, L., Jurak, E., Deuss, P.J., Barta, K., 2021. Tunable and functional deep eutectic solvents for lignocellulose valorization. *Nat Commun* 12. <https://doi.org/10.1038/s41467-021-25117-1>
- Lobato-Peralta, D.R., Duque-Brito, E., Villafán-Vidales, H.I., Longoria, A., Sebastian, P.J., Cuentas-Gallegos, A.K., Arancibia-Bulnes, C.A., Okoye, P.U., 2021. A review on trends

- in lignin extraction and valorization of lignocellulosic biomass for energy applications. *J Clean Prod.* <https://doi.org/10.1016/j.jclepro.2021.126123>
- Lobato-Rodríguez, Á., Gullón, B., Romaní, A., Ferreira-Santos, P., Garrote, G., Del-Río, P.G., 2023. Recent advances in biorefineries based on lignin extraction using deep eutectic solvents: A review. *Bioresour Technol* 388. <https://doi.org/10.1016/j.biortech.2023.129744>
- Lou, R., Zhang, X., 2022. Evaluation of pretreatment effect on lignin extraction from wheat straw by deep eutectic solvent. *Bioresour Technol* 344. <https://doi.org/10.1016/j.biortech.2021.126174>
- Lourenço, A., Rencoret, J., Chemetova, C., Gominho, J., Gutiérrez, A., Del Río, J.C., Pereira, H., 2016. Lignin composition and structure differs between Xylem, Phloem and phellem in quercus suber L. *Front Plant Sci* 7. <https://doi.org/10.3389/fpls.2016.01612>
- Luo, X., Li, Y., Gupta, N.K., Sels, B., Ralph, J., Shuai, L., 2020. Protection Strategies Enable Selective Conversion of Biomass. *Angewandte Chemie - International Edition.* <https://doi.org/10.1002/anie.201914703>
- Luo, Z., Qian, Q., Sun, H., Wei, Q., Zhou, J., Wang, K., 2023. Lignin-First Biorefinery for Converting Lignocellulosic Biomass into Fuels and Chemicals. *Energies (Basel).* <https://doi.org/10.3390/en16010125>
- Mujtaba, M., Fernandes Fraceto, L., Fazeli, M., Mukherjee, S., Savassa, S.M., Araujo de Medeiros, G., do Espírito Santo Pereira, A., Mancini, S.D., Lipponen, J., Vilaplana, F., 2023. Lignocellulosic biomass from agricultural waste to the circular economy: a review with focus on biofuels, biocomposites and bioplastics. *J Clean Prod.* <https://doi.org/10.1016/j.jclepro.2023.136815>
- Provost, V., Dumarcay, S., Ziegler-Devin, I., Boltoeva, M., Trébouet, D., Villain-Gambier, M., 2022. Deep eutectic solvent pretreatment of biomass: Influence of hydrogen bond donor and temperature on lignin extraction with high β -O-4 content. *Bioresour Technol* 349. <https://doi.org/10.1016/j.biortech.2022.126837>
- Ragauskas, A.J., Beckham, G.T., Biddy, M.J., Chandra, R., Chen, F., Davis, M.F., Davison, B.H., Dixon, R.A., Gilna, P., Keller, M., Langan, P., Naskar, A.K., Saddler, J.N., Tschaplinski, T.J., Tuskan, G.A., Wyman, C.E., 2014. Lignin valorization: Improving lignin processing in the biorefinery. *Science* (1979). <https://doi.org/10.1126/science.1246843>
- Ralph, J., Lapierre, C., Boerjan, W., 2019. Lignin structure and its engineering. *Curr Opin Biotechnol.* <https://doi.org/10.1016/j.copbio.2019.02.019>
- Renders, T., Van Den Bosch, S., Koelewijn, S.F., Schutyser, W., Sels, B.F., 2017. Lignin-first biomass fractionation: The advent of active stabilisation strategies. *Energy Environ Sci.* <https://doi.org/10.1039/c7ee01298e>
- Rodrigues, B.G., José, Á.H.M., Prado, C.A., Rodrigues, D., Rodrigues, R.C.L.B., 2024. Optimizing corn cob pretreatment with eco-friendly deep eutectic solvents to enhance lignin extraction and cellulose-to-glucose conversion. *Int J Biol Macromol* 283. <https://doi.org/10.1016/j.ijbiomac.2024.137432>
- Rodrigues, J.S., Lima, V., Araújo, L.C.P., Botaro, V.R., 2021. Lignin Fractionation Methods: Can Lignin Fractions Be Separated in a True Industrial Process? *Ind Eng Chem Res.* <https://doi.org/10.1021/acs.iecr.1c01704>

- Roy, R., Rahman, M.S., Amit, T.A., Jadhav, B., 2022. Recent Advances in Lignin Depolymerization Techniques: A Comparative Overview of Traditional and Greener Approaches. *Biomass (Switzerland)*. <https://doi.org/10.3390/biomass2030009>
- Ruwoldt, J., Blindheim, F.H., Chinga-Carrasco, G., 2023. Functional surfaces, films, and coatings with lignin - a critical review. *RSC Adv*. <https://doi.org/10.1039/d2ra08179b>
- Sethupathy, S., Murillo Morales, G., Gao, L., Wang, H., Yang, B., Jiang, J., Sun, J., Zhu, D., 2022. Lignin valorization: Status, challenges and opportunities. *Bioresour Technol*. <https://doi.org/10.1016/j.biortech.2022.126696>
- Stiefel, S., Lölsberg, J., Kipshagen, L., Möller-Gulland, R., Wessling, M., 2015. Controlled depolymerization of lignin in an electrochemical membrane reactor. *Electrochem commun* 61, 49–52. <https://doi.org/10.1016/j.elecom.2015.09.028>
- Sun, Z., Fridrich, B., De Santi, A., Elangovan, S., Barta, K., 2018. Bright Side of Lignin Depolymerization: Toward New Platform Chemicals. *Chem Rev*. <https://doi.org/10.1021/acs.chemrev.7b00588>
- Tian, Z., Zong, L., Niu, R., Wang, X., Li, Y., Ai, S., 2015. Recovery and characterization of lignin from alkaline straw pulping black liquor: As feedstock for bio-oil research. *J Appl Polym Sci* 132. <https://doi.org/10.1002/APP.42057>
- Wang, H., Tucker, M., Ji, Y., 2013. Recent Development in Chemical Depolymerization of Lignin: A Review. *Journal of Applied Chemistry* 2013, 1–9. <https://doi.org/10.1155/2013/838645>
- Wang, Y., Liu, Q., Yan, C., Song, G., Price, W.S., Zheng, G., Torres, A.M., Xue, Z., 2025. Deep eutectic solvent-driven mild lignocellulose pretreatment: Unlocking lignin valorization and carbohydrate digestibility. *Chemical Engineering Journal* 504. <https://doi.org/10.1016/j.cej.2024.158825>
- Wang, Y.-Y., Cai, C.M., Ragauskas, A.J., n.d. Recent Advances in Lignin-based Polyurethanes.
- Wang, Z., Deuss, P.J., 2023. The isolation of lignin with native-like structure. *Biotechnol Adv*. <https://doi.org/10.1016/j.biotechadv.2023.108230>
- Xiao, T., Hou, M., Guo, X., Cao, X., Li, C., Zhang, Q., Jia, W., Sun, Y., Guo, Y., Shi, H., 2024. Recent progress in deep eutectic solvent(DES) fractionation of lignocellulosic components : A review. *Renewable and Sustainable Energy Reviews*. <https://doi.org/10.1016/j.rser.2023.114243>
- Xu, R., Zhang, K., Liu, P., Han, H., Zhao, S., Kakade, A., Khan, A., Du, D., Li, X., 2018. Lignin depolymerization and utilization by bacteria. *Bioresour Technol*. <https://doi.org/10.1016/j.biortech.2018.08.118>
- Yousuf, A., Pirozzi, D., Sannino, F., 2019. Fundamentals of lignocellulosic biomass, in: *Lignocellulosic Biomass to Liquid Biofuels*. Elsevier, pp. 1–15. <https://doi.org/10.1016/B978-0-12-815936-1.00001-0>
- Zhang, C.W., Xia, S.Q., Ma, P.S., 2016. Facile pretreatment of lignocellulosic biomass using deep eutectic solvents. *Bioresour Technol* 219, 1–5. <https://doi.org/10.1016/j.biortech.2016.07.026>
- Zhang, H., Shi, Y., Li, M., Chen, J., Xin, Y., Zhang, L., Gu, Z., Liu, J., Liu, R., 2022. Extraction of lignin from corncob residue via a deep eutectic solvent for the preparation of

- nanoparticles by self-assembly. Chem Eng Sci 256.
<https://doi.org/10.1016/j.ces.2022.117694>
- Zhang, L., Yu, H., Liu, S., Wang, Y., Mu, T., Xue, Z., 2023a. Kamlet-Taft Parameters of Deep Eutectic Solvents and Their Relationship with Dissolution of Main Lignocellulosic Components. Ind Eng Chem Res 62, 11723–11734.
<https://doi.org/10.1021/acs.iecr.3c01309>
- Zhang, L., Yu, H., Liu, S., Wang, Y., Mu, T., Xue, Z., 2023b. Kamlet-Taft Parameters of Deep Eutectic Solvents and Their Relationship with Dissolution of Main Lignocellulosic Components. Ind Eng Chem Res 62, 11723–11734.
<https://doi.org/10.1021/acs.iecr.3c01309>
- Zhang, S., Xiao, J., Wang, G., Chen, G., 2020. Enzymatic hydrolysis of lignin by ligninolytic enzymes and analysis of the hydrolyzed lignin products. Bioresour Technol 304.
<https://doi.org/10.1016/j.biortech.2020.122975>
- Zhang, Z., 2022. Making the Most of Lignin by Catalytic Depolymerization. University of Groningen. <https://doi.org/10.33612/diss.211888420>